ČESKÉ VYSOKÉ UČENÍ TECHNICKÉ V PRAZE

FAKULTA ELEKTROTECHNICKÁ

BAKALÁŘSKÁ PRÁCE

Automatická detekce a analýza elektrických zátěží v průmyslových řídicích I/O systémech

Automatic detection and analysis of electrical loads in industrial control I/O systems

2024

Marek Novotný

Studijní program: Elektrotechnika, elektronika a komunikační technika

Vedoucí práce: prof. Ing. Miroslav Husák, CSc.

NOVOTNÝ, MAREK. *Automatic detection and analysis of electrical loads in industrial control I/O systems*. Praha: ČVUT 2024. Bakalářská práce. České vysoké učení technické v Praze, Fakulta elektrotechnická.

FAKULTA
ELEKTROTECHNICKÁ
ČVUT V PRAZE

Prohlášení

Prohlašuji, že jsem svou bakalářskou práci vypracoval(a) samostatně. Dále prohlašuji, že jsem všechny použité zdroje správně a úplně citoval(a) a uvádím je v přiloženém seznamu použité literatury.

Nemám závažný důvod proti zpřístupňování této závěrečné práce v souladu se zákonem č. 121/2000 Sb., o právu autorském, o právech souvisejících s právem autorským a o změně některých zákonů (autorský zákon) v platném znění.

V Praze dne: 09. 01. 2024 Podpis:

ZADÁNÍ BAKALÁŘSKÉ PRÁCE

I. OSOBNÍ A STUDIJNÍ ÚDAJE

Příjmení: **Novotný** Jméno: **Marek** Osobní číslo: **466011**

Fakulta/ústav: **Fakulta elektrotechnická**

Zadávající katedra/ústav: **Katedra mikroelektroniky**

Studijní program: **Elektrotechnika, elektronika a komunikační technika**

II. ÚDAJE K BAKALÁŘSKÉ PRÁCI

Název bakalářské práce:

Automatická detekce a analýza elektrických zátěží v průmyslových řídicích I/O systémech

Název bakalářské práce anglicky:

Automatic Detection and Analysis of Electrical Loads in Industrial Control I/O Systems

Pokyny pro vypracování:

1. Shrňte poznatky o průmyslových standardech pro řídicí systémy, poznatky o řízení digitálních akčních členů v průmyslové automatizaci a soudobých aplikacích prediktivní údržby v systémech digitálních vstupů a výstupů (I/O). Zhodnoťte možnosti realizace prediktivní údržby v oblasti řízení digitálních vstupů a výstupů pomocí dostupných integrovaných obvodů.
2. Navrhněte technické řešení automatické detekce a analýzy parametrů elektrických zátěží (aktuátorů) řízených standardními průmyslovými digitálními I/O systémy. Navrhněte algoritmy a obvodová řešení s pomocí obvodů řady IPS (Intelligent Power Switches) od firmy STMicroelectronics. Pro návrh využijte digitální I/O modul STEVAL-FSM01M1 v součinnosti s deskou NUCLEO-F401RE osazenou mikrokontrolérem STM32F401RE, a případně navrhněte jeho možné modifikace.
3. Dosažené výsledky a navrhovaná řešení shrňte v závěru práce, práci vypracujte v anglickém jazyce.

Seznam doporučené literatury:

1. J. D. Irwin, Basic Engineering Circuit Analysis. S.l.: Wiley, 2020.
2. V. Haasz, J. Holub, M. Janošek, P. Kašpar, and V. Petrucha, Elektrická Měření: Přístroje a Metody. Praha: Česká technika - nakladatelství ČVUT, 2018.
3. IEC 61131-2 Industrial-Process Measurement And Control - Programmable Controllers - Part 2: Equipment Requirements and Tests.

Jméno a pracoviště vedoucí(ho) bakalářské práce:

prof. Ing. Miroslav Husák, CSc. katedra mikroelektroniky FEL

Jméno a pracoviště druhé(ho) vedoucí(ho) nebo konzultanta(ky) bakalářské práce:

Datum zadání bakalářské práce: **26.09.2023** Termín odevzdání bakalářské práce: **09.01.2024**

Platnost zadání bakalářské práce: **21.09.2025**

prof. Ing. Miroslav Husák, CSc. podpis vedoucí(ho) práce	prof. Ing. Pavel Hazdra, CSc. podpis vedoucí(ho) ústavu/katedry	prof. Mgr. Petr Páta, Ph.D. podpis děkana(ky)

III. PŘEVZETÍ ZADÁNÍ

Student bere na vědomí, že je povinen vypracovat bakalářskou práci samostatně, bez cizí pomoci, s výjimkou poskytnutých konzultací. Seznam použité literatury, jiných pramenů a jmen konzultantů je třeba uvést v bakalářské práci.

. | Datum převzetí zadání

Podpis studenta

Poděkování

Tímto chci poděkovat týmu pražské laboratoře STMicroelectronics kde mi poskytli zázemí pro návrh a měření k této práci. Dále chci poděkovat panu profesorovi Miroslavu Husákovi, který se ujal vedení této práce.

Abstrakt

Cílem této práce bylo nalézt technické řešení pro automatickou detekci a spínání průmyslových aktuátorů a stanovení jejich parametrů odporu, indukčnosti a kapacity pomocí analýzy napěťových a proudových signálů. Studie zahrnovala seznámení s průmyslovými akčními členy, vyhodnocení hardwarové proveditelnosti, návrh měřeného vzorku a provedení měřicích experimentů. Výsledky zahrnují dvě detekční metody založené na hardwarovém návrhu a poměrech ploch ohraničených analyzovanými signály použité k implementaci dvou detekčních algoritmů, spolu se sedmi algoritmy implementujícími různé metody určování parametrů. Navrhovaná vylepšení zahrnují integraci sekce pro měření proudu do hardwarového návrhu a zvážení analýzy frekvenční domény pro budoucí iterace.

Klíčová slova

prediktivní údržba, detekce zátěže, analýza parametrů zátěže, vstupně-výstupní elektronika, řídicí elektronika, průmyslové řízení

Abstract

This work aimed to find a technical solution for the automatic detection and switching of industrial actuators and determining their resistance, inductance, and capacitance parameters by analyzing voltage and current signals. The study involved familiarizing with industrial actuators, evaluating hardware feasibility, designing a measurement sample, and conducting measurement experiments. The results include two detection methods based on hardware design and ratios of areas traced out by analyzed signals used to implement two detection algorithms, along with seven algorithms implementing different parameter determination methods. Suggested improvements include integration of a current measuring section in hardware design and consideration of frequency domain analysis for future iterations.

Keywords

predictive maintenance, load detection, load parameter analysis, input-output electronics, electronic control, industrial control

Contents

Nomenclature

Symbols	Base Unit	Description
a, b, c, d	-	General purpose parameters
x, y	-	General purpose variables
C_1	*Farad (F)*	Load capacitance
e	-	Euler's number
E	*Joule (J)*	Total energy
E_{DEMAG}	*Joule (J)*	Energy dissipated inside a load during demagnetization
E_{INFLUX}	*Joule (J)*	Energy stored in a magnetic field
E_{INRUSH}	*Joule (J)*	Energy stored in an electric field or turned into incandescent heat and radiation
E_R	*Joule (J)*	Energy dissipated in a resistance
E_{SWITCH}	*Joule (J)*	Energy dissipated inside a switch during demagnetization
G_1	*Siemens (S)*	Load conductance
i	*Ampere (A)*	Switched output current
I	*Ampere (A)*	Current in Laplace transform
I_0	*Ampere (A)*	Initial current amplitude
I_1	*Ampere (A)*	Switched current steady-state amplitude
I_{bias}	*Ampere (A)*	Mean optocoupler diode bias current
I_{DECAY}	*Ampere (A)*	Current bias of exponential decay term
$I_{FH(min)}$ $I_{FH(max)}$	*Ampere (A)*	Optocoupler diode active forward current (minimum, maximum)
L_1	*Henry (H)*	Load inductance
P_{DEMAG}	*Watt (W)*	Power dissipation inside a load during demagnetization
P_{INFLUX}	*Watt (W)*	Power flow into a magnetic field

Symbols	Base Unit	Description
P_{INRUSH}	*Watt (W)*	Power flow into an electric field or incandescent heat and radiation
P_{SWITCH}	*Watt (W)*	Power dissipation inside a switch during demagnetization
P_{STEADY}	*Watt (W)*	Power dissipation inside a load in a steady state
Q	*Coulomb (C)*	Charge under exponential current growth
q	*Coulomb (C)*	Difference between equivalent steady state charge and charge under current growth
R^2	-	Coefficient of determination
R_0	*Ohm (Ω)*	Switch output resistance
R_1	*Ohm (Ω)*	Load resistance
R_{bias}	*Ohm (Ω)*	Mean optocoupler diode bias resistance
R_{COLD}	*Ohm (Ω)*	Resistance at room temperature
$R_{EFFECTIVE}$	*Ohm (Ω)*	Equivalent effective resistance of a transient
s	*Hertz (Hz)*	Complex frequency symbol in Laplace transform
t	*Second (s)*	Time parameter
T	*Second (s)*	General purpose time interval duration
T_{DEMAG}	*Second (s)*	Duration demagnetization of inductive load
$T_{OVERLOAD}$	*Second (s)*	Duration of initial high current demand
T_{STEADY}	*Second (s)*	Time to reach a steady state
u	-	Unit step function
v_1	*Volt (V)*	Switch output voltage
v_{DECAY}	*Volt (V)*	Exponential voltage decay
v_{GROWTH}	*Volt (V)*	Exponential voltage growth
v_R	*Volt (V)*	Voltage across resistance
v_{RC}	*Volt (V)*	Voltage across capacitive load
v_L	*Volt (V)*	Voltage across inductance

Symbols	Base Unit	Description
V_0	*Volt (V)*	Initial voltage amplitude
V_1	*Volt (V)*	Switched voltage steady-state amplitude
V_{bias} $V_{bias(min)}$ $V_{bias(max)}$	*Volt (V)*	Optocoupler diode bias voltage (mean, minimum, maximum)
$V_{BR(min)}$ $V_{BR(max)}$	*Volt (V)*	Transil diode breakdown voltage (minimum, maximum)
V_{CC} $V_{CC(max)}$	*Volt (V)*	Voltage source (mean and maximum)
$V_{CLAMP(max)}$ $V_{CLAMP(min)}$	*Volt (V)*	Switch demagnetization clamping voltage (maximum, minimum)
V_{DEMAG} $V_{DEMAG(max)}$ $V_{DEMAG(min)}$	*Volt (V)*	Voltage across load during demagnetization (mean, maximum, minimum)
V_F	*Volt (V)*	Optocoupler diode forward voltage drop
V_{RC}	*Volt (V)*	Voltage across a capacitive load in Laplace transform
V_{RM}	*Volt (V)*	Transil diode standoff voltage
θ	*°C*	Temperature
τ	*Second (s)*	Time constant
σ	-	Integral area ratio

Introduction

My thesis explores analytic methods of load detection and determination of load parameters in the context of the field of predictive maintenance of industrial equipment such as actuators, bulbs, brakes, and more generally other types of loads with their specific parameters.

Contribution of such methods is the ability to extract the fundamental electrical parameters from observation of the driving signals mainly voltage and current to be used in further predictive maintenance endeavors such as tracking of drifting load parameters in time as an indicator of potential wear of monitored components which usually endure thermal, mechanical and electrical stress in industrial applications. Such indicator could be further used in short and long-term data analyses which could give an early warning signal of component's wear and may help in maintenance scheduling.

This work is anchored in a more general topic of predictive maintenance which is a field that studies when a given component might fail by acquisition of data produced by the component and using data analysis throughout time to determine if there are any deviations in the behavior predicting component's wear or failure.

Benefit of this approach to maintenance is an optimization of downtime of industrial processes which in this case would be stopped when it is absolutely necessary possibly lengthening the time between maintenance periods and making planning around maintenance cycles easier.

The literature on this subject is mostly in two categories. First, a literature of general introduction and second a literature exploring more conceptual, abstract, and somewhat advanced techniques of data processing through the usage of machine learning and advanced statistics. Some of these sources will be reviewed in the theoretical introduction of this work. A Large part of my work on the other hand will entail more straightforward techniques, methods, and approaches revolving around measurement and concrete technical solutions which will lead to a more practical exploration of the subject.

The goal of this work is to put various methods to the test by considering the evaluation board STEVAL-FSM01M1 by STMicroelectronics fitted with components targeting industrial control and automation as an exemplary target environment and if deemed unsuitable for the task create or revise a new hardware design.

In summary, the results of this work should be a modified or new hardware design including suggestions for improvement to older designs. A multitude of methods for detecting the type of switched load and for computing the fundamental parameters of switched load. This includes any auxiliary methods enabling other methods to function properly. The methods then will be used to build a bulk of algorithmic solutions outlining execution order implementing the derived methods.

THEORETICAL SECTION

1 Past and current approaches

My work is created in the context of predictive maintenance which is still a new and changing environment where experimentation still outweighs practice but the general paradigm is known. This paradigm evolved over time from previous ones and it bares to talk about older iterations of maintenance practice to put things into perspective and show what is new with the predictive approach as it clears up a lot about the purpose of this work and introduces the designated environment for this work.

Maintenance as a more systematic technical topic started at the time of the Industrial Revolution and the development of mass production. The oldest and most rudimentary approach to maintenance is reactive. This means that maintenance is carried out as a reaction to the equipment breakdown. This approach was sufficient in early industrial manufacturing when consequences of unexpected downtime were limited and resulting costs manageable with simpler industrial equipment. The two advantages of this approach are its ease of implementation and low intermediary costs but disadvantages are numerous including unknown maintenance schedule, possibly longer and more costly repairs, no organized strategy for preventing downtime, and the only improvement to be made is sourcing and testing the parts for the best reliability track record. The next distinctive shift happened in the second half of the twentieth century after the war period with the beginning of more global industrial cooperation and the move to automated manufacturing. This new approach was preventive where each part of industrial equipment was assigned a lifespan and at the end of this lifespan, it was replaced irrespective of its true condition. The advantages of this new approach are immediately apparent when we compare them with reactive maintenance. In this case, elementary prevention measures are applied by considering new parts as more reliable and assigning a date for a replacement of each part which already constitutes a basic strategy and planning. The maintenance schedule is guided by the replacement dates of components. Replacing components on time results in less serious damage or avoids it altogether which leads to lower repair costs and less downtime. This process of course comes with more management overhead and higher intermediary costs but these setbacks are usually outweighed by more consistent production. Improvements can be achieved in a very similar way to reactive maintenance by measuring and testing parts and determining the ones that take the longest to fail.

This is where predictive maintenance offers an advantage because it adds direct real-time monitoring of components and uses acquired data to create a model rating their condition. This should allow for more accurate decision making as it allows to take direct advantage of measured physical signals which give information about true physical state and condition. Since factories are becoming full of sensors that produce a lot of data. Predictive maintenance should be the tool to make sense of this. However, it seems that it is still a semi-novel technology not yet completely solidified in the industrial zeitgeist so to speak because of a lot of basic introduction literature from recent years. This includes technical news and presentations by consultation agencies [1]–[6] generally in the vein of simple concept introduction and preliminary economic and business considerations. A lot of articles also provide only introduction and propose high-level architecture for predictive maintenance systems [7]–[12]. The biggest analysis tools are indisputably data science and machine learning approaches [13]–[23] usually used together with some kind of IIoT system. Even though there are direct applications in these articles they mostly revolve around analysis of machinery.

1.1 Enabling technology and hardware

Semiconductor manufacturers provide a generous selection of components implementing technologies either directly targeted at predictive maintenance or for a general industrial automation use case. This includes isolators for digital input and output, all manners of industrial micro-controller units, various signal sampling and processing units, and communication interfaces. Some companies even offer whole ready-made platforms.[24], [25] Instead of listing the sea of standalone components I will list a few reference designs in tab. 1 related to my goal in this work and maybe in some aspects can complement the hardware available to me.

TAB. 1: REFERENCE DESIGNS AND EVALUATION BOARDS SHOWCASE

Board reference	Manufacturer	Description
EVM430-I2040S	Texas Instruments	Board capable of metering a multitude of power, current, and voltage signals [26]
TIPD121	Texas Instruments	Reference design for 5-A, 2-kV isolated current sensing [27]
CN0549	Analog Devices	Reference design for condition-based monitoring development platform [28]
TIDA-01552	Texas Instruments	Digital output high-side switch reference design [29]
REF-ISOH812G-I813T	Infineon Technologies	Industrial IO board [30]
KITVALVECNTLEVM	NXP Semiconductors	Board for control of valves [31]
STEVAL-BFA001V2B	STMicroelectronics	Multi-sensor predictive maintenance kit [32]
MAXREFDES278	Maxim Integrated	IO-Link solenoid actuator board [33]
EVAL-ADMX2001	Analog Devices	High-Performance Precision Impedance Analyzer Measurement Module [34]

When weighing the possibilities nothing is preventing me from continuing with the rest of the work since the offering includes so many feature-rich components. Since I will need only a common kind of hardware functionalities it would be completely feasible to put together the hardware with available components. It would also be possible to put together a hardware design that would be a part of a larger predictive maintenance system this would probably only need an addition of a communication interface to integrate it into the system. The advantages of such integration would be a knowledge of characteristic parameters of switched loads and their tracking by the predictive maintenance system much like was described above.

2 Foundation

The goal of this work is to create a solution for the automatic detection of some common industrial load parameters. Here I will lay out the founding theory of my work and the methods I will take to solve this problem. This work will focus on resistive, inductive and capacitive loads as they represent very commonplace industrial actuators. When researching detection methods and modeling of typical loads I only came across a somewhat relevant paper [35] which is still too out of the niche of this work therefore I will stick to my own devices.

2.1 Scope of work and methodology

The scope of this work will be an exploration of what happens when an unknown load is connected to a smart switching device with the IPS1025H high-side switch with diagnostics for overload conditions and thermal protection. The core objective will be measurements of resulting signals at the output of the switching device when the connected load is switched on and off. These measurements will serve as a basis for the creation of basic decision algorithms for the detection of connected load and its parameters.

To firmly delineate the course of this work I will provide readers with this checklist of premises to contextualize my approach to the work

i. The nature of the inner structure of a connected load is considered unknown
ii. Expected natural responses of load models are illustrated with simulation. For the sake of comparison with application-specific responses further measurements can be taken.
iii. Application-specific response parameters are thoroughly measured and analyzed. Measured waveforms are saved for calculation purposes.
iv. The analysis is done on digital actuators and digital in nature with high and low switching voltage levels.
v. The analysis is built on the elementary passive components of resistivity, capacitance, and inductance
vi. The analysis is done from a view of the smart switching device and as such purely electrical in nature without crossing into other domains e. g. mechanical. This work does not provide mixed models.
vii. Only models of actuators that are commonly used in the industry and have clearly outlined desirable parameters are the subject of this work. These could include all kinds of windings (speaker, transformer, etc.), resistive heating elements, strain gauges, solenoid valves, general electronic load, etc. [36]
viii. Loads operating with inherently variable resistivity, capacitance, or inductance might be possible to analyze. It is not however the main objective of this work and will not be guaranteed.

2.2 Theory

Based on the previously mentioned premises providing a skeleton for the work which starts with the assumption that the inner design of a load is unknown and can be modeled with resistivity, inductance, and capacitance. Since the load has to have a clear digital state with some sort of well-defined rising and falling edges to the signal responses it is clear that a combination of all the above elements is undesirable due to the signal oscillations inherent to a circuits including both capacitors and inductors. That leaves only resistive, inductive, and capacitive circuit models left. It is important to brush up on the theory and behavior of these circuits as it will prove instrumental in deciding the type of load and determination of its parameters. This section will lay out the theory and behavior of DC signals in resistive, inductive, and capacitive loads.

2.2.1 Resistive load

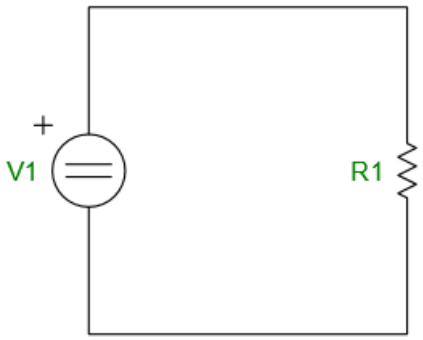

FIGURE 1: CIRCUIT DIAGRAM OF RESISTIVE LOAD

Simulation in Figure A.1 shows the characteristic behavior of resistive loads. There is no lag between voltage and current both signals step up and step down at the same time. This relation can be put into formula form by examining the circuit in Figure 1 with Kirchoff's and Ohm's laws (1).

$$v_1(t) - v_R(t) = 0 \Rightarrow v_1(t) - R_1 \cdot i(t) = 0 \quad (1)$$

$$i(t) = \frac{v_1(t)}{R_1} = G_1 \cdot v_1(t) \quad (2)$$

When solving for current (2) it is apparent that current is directly proportional to the voltage of the supply. This relationship can be used to analyze purely resistive loads. In terms of industrial actuators that can be modeled by purely resistive load usually are exclusively resistive heating elements.

2.2.2 Inductive load

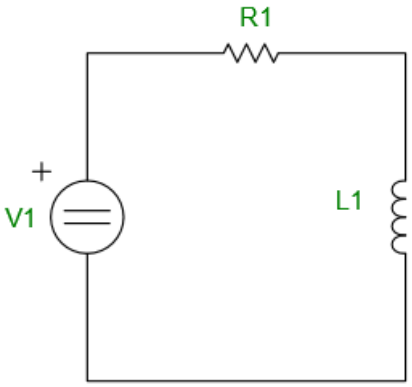

FIGURE 2: CIRCUIT DIAGRAM OF INDUCTIVE LOAD

Simulation in Figure A.2 shows the characteristic behavior when switching an inductive load. It matches the well-known transient behavior of first-order inductive circuit. Switching inductance on causes voltage to rise across inductor in opposition to the current direction and the energy provided from the source gets transformed into thermal losses and the magnetic field of the inductor. When a steady state is reached and the voltage across the inductor subsides then the inductor is equivalent to a short circuit. Switching the inductance off causes a voltage to rise across the inductor in accordance with the current direction and the inductor momentarily becomes a secondary source of energy within the circuit until its energy is dissipated to thermal losses.

This behavior can be expressed with a formula by examining the circuit in Figure 2 with Kirchhoff's, Ohm's, and Faraday-Lenz's laws and then solving resulting differential equations. In this case, I will use Laplace transform the circuit to find the solution to the step response.

$$v_1(t)-v_R(t)-v_L(t)=v_1(t)-R_1\cdot i(t)-L_1\cdot\frac{d\,i(t)}{dt}=0\Rightarrow V_1\cdot u(t)-R_1\cdot i(t)-L_1\cdot\frac{d\,i(t)}{dt}=0 \qquad (3)$$

$$\mathscr{L}\left[V_1\cdot u(t)-R_1\cdot i(t)-L_1\cdot\frac{d\,i(t)}{dt}\right]=0\Rightarrow\frac{V_1}{s}-R_1\cdot I(s)-L_1\cdot(s\cdot I(s)-i(0))=0 \qquad (4)$$

$$\mathscr{L}^{-1}\left[I(s)=\frac{V_1}{L_1}\cdot\frac{1}{s\cdot(s+R_1/L_1)}+i(0)\cdot\frac{1}{s+R_1/L_1}\right]\Rightarrow i(t)=\frac{V_1}{R_1}+\left(I_0-\frac{V_1}{R_1}\right)e^{(-R_1t/L_1)}, \qquad (5)$$

$$I_0=i(t=0),V_1=v_1(t\to\infty)$$

After the transformation of the voltage equation (3) to (4) it is possible to solve for current in the circuit by inverse transform (5). This solution gives the general formula for the current through inductive load. Voltages can be obtained easily by substituting the current solution to the expressions relating current with voltage for the rest of the components. In terms of industrial actuators that can be modeled by inductive load include solenoid valves, relays, contactors, reed switches, induction heaters, stepper motors, etc.

2.2.3 Capacitive load

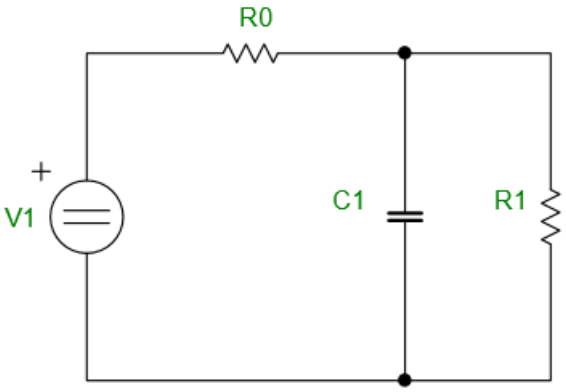

FIGURE 3: CIRCUIT DIAGRAM OF CAPACITIVE LOAD

Simulation in Figure A.3 shows the characteristic behavior when switching a capacitive load. Here I opted for a more hybrid approach to the analysis of the load since there can be two types of capacitive loads one that draws current only to charge itself which is not that common but could be represented by a purely electrostatic actuator but even then it is hard to imagine that there would not be an attached auxiliary electronic control sinking some amount of current therefore the other more common would be a load that has some initial capacitance that needs to be charged but in the steady state draws constant current this can represent majority of electronic devices used in the industry with semiconductor and resistive components drawing power and this case will be explored further in this work. Another advantage to this setup is a general model which can be parametrized for both cases and can even simulate switch off by changing resistances to open circuits or short circuits. Switching capacitance on causes charging current to flow through the circuit into the capacitor and voltage across capacitor plates starts to rise. With time less charging current flows to the capacitor while equivalent resistive load current picks up and when a steady state is reached then voltage across the capacitor matches that of a supply circuit and resistive load is all that remains. When the capacitive load is switched off the energy stored in it causes current to flow in the opposite direction to the charging current this energy dissipates in the surrounding resistive elements until voltage across the capacitor goes to zero.

The formula for the behavior of this circuit is obtained by examining the circuit in Figure 3 by using Kirchoff's and Ohm's laws as well as the relation between voltage and current of a capacitor and solving the system of differential equations.

$$\begin{gathered} v_1(t) - R_0 \cdot i(t) - v_{RC}(t) = 0 \\ v_{RC}(t) - R_1 \cdot i_1(t) = 0 \\ \Rightarrow v_{RC}(t)\frac{R_0+R_1}{R_0} + R_1 C_1 \cdot \frac{d\,v_{RC}(t)}{dt} - v_1(t)\frac{R_1}{R_0} = 0 \end{gathered} \tag{6}$$

$$\begin{gathered} \mathscr{L}\left[v_{RC}(t)\frac{R_0+R_1}{R_0} + R_1 C_1 \cdot \frac{d\,v_{RC}(t)}{dt} - V_1 \cdot u(t)\frac{R_1}{R_0} \right] = 0 \\ \Rightarrow V_{RC}(s)\frac{R_0+R_1}{R_0} + R_1 C_1 \cdot (s \cdot V_{RC}(s) - v_{RC}(0)) - \frac{V_1}{s}\frac{R_1}{R_0} = 0 \end{gathered} \tag{7}$$

$$\mathscr{L}^{-1}\left[V_{RC}(s)=\frac{1}{s\cdot\left(s+\frac{R_0+R_1}{R_0\cdot R_1\cdot C_1}\right)}\cdot\frac{V_1}{R_0\cdot C_1}+\frac{1}{s+\frac{R_0+R_1}{R_0\cdot R_1\cdot C_1}}V_0 \right] \quad (8)$$

$$\Rightarrow v_{RC}(t)=V_1\frac{R_1}{R_0+R_1}+\left(V_0-V_1\frac{R_1}{R_0+R_1}\right)e^{-\frac{R_0+R_1}{R_0\cdot R_1\cdot C_1}t},$$

$$V_0=v_{RC}(t=0), V_1=v_1(t\to\infty)$$

After the transformation of the voltage equation (6) to (7) it is possible to solve for the voltage at the output of the circuit by inverse transform (8). This voltage can be used to figure out currents in the rest of the circuit. Now it is possible to simplify for the outlined cases of capacitive loads.

$$\lim_{R_0\to 0} v_{RC}(t)=V_1, V_1=v_1(t\to\infty) \quad (9)$$

$$\lim_{R_1\to\infty} v_{RC}(t)=V_1+(V_0-V_1)e^{-\frac{t}{R_0C_1}}, V_0=v_{RC}(t=0), V_1=v_1(t\to\infty) \quad (10)$$

By taking the proper limits of the previous formula (8) it is possible to get the formula for the purely chargeable capacitive load (9) and capacitive load with a constant draw (10). These equations are useful when analyzing different types of capacitive loads. In terms of industrial actuators capacitive loads represent general electronic devices.

TECHNICAL SOLUTION

3 Solution process

To approach the technical solution of the issue I will start with an abstract model of how an electronic device might be able to detect and determine parameters of different types of loads and on this basis I will devise a process to achieve the solution.

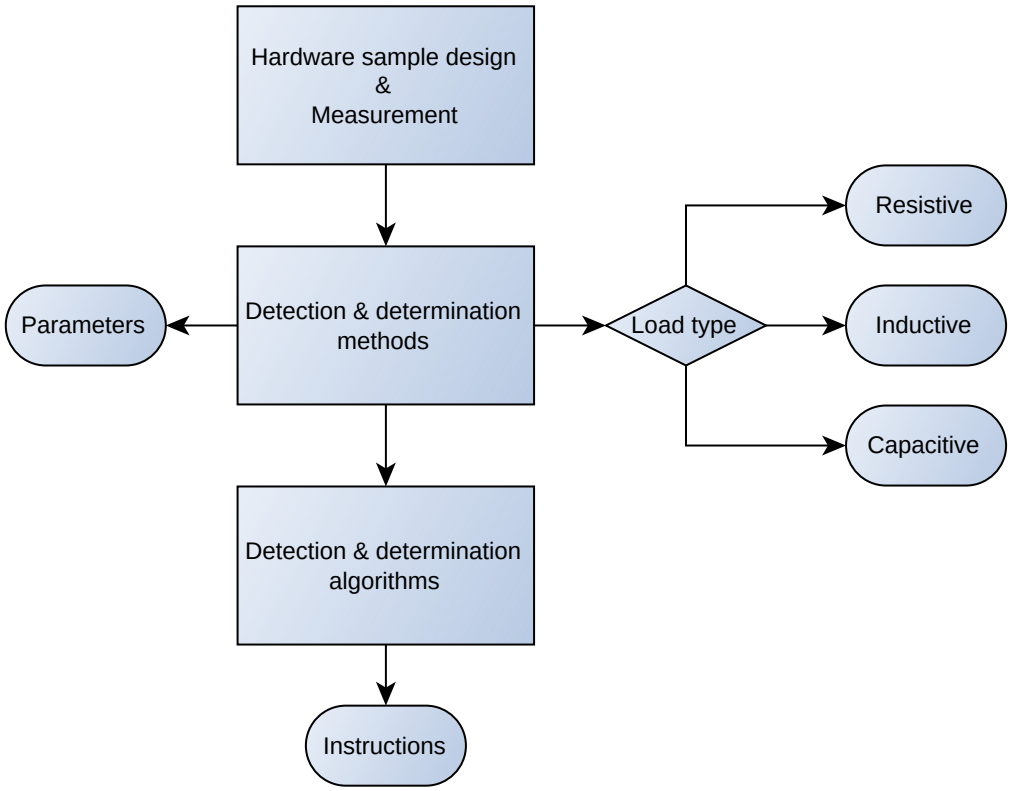

FIGURE 4: TECHNICAL SOLUTION OVERVIEW

The diagram in Figure 4 represents all the necessary tasks to achieve the technical solution of load type detection and load parameter determination. This solution overview will serve as a template for the upcoming chapters.

To summarize the structure of this section. Firstly I need a device to do easy measurements with easy access to signal probing. I have the STEVAL-FSM01M1 [37] evaluation board already at hand with easy access to test points and an analog-to-digital converter for capturing the output signal of the board. However, it has limited diagnostic to the switching of the connected loads. Therefore I will design a second evaluation board with more advanced high side switch IPS1025H by STMicroelectronics that has smart features for driving capacitive and inductive loads with diagnostic signalization. The hardware design process utilizing OrCAD PCB design software suite will be summarized in one chapter.

Results should introduce methods and algorithms that can detect the type of the connected load and determine its parameters. Methods will explore the theoretical side of the solution whereas algorithms will give simply an execution order of instructions implementing each method. Both detection and determination algorithms and methods will be devised for each type of tested load and summarized in their own chapters.

4 Smart switch device design

The result of this design will be an evaluation board which will serve as the main measurement sample for my work. Even though the STEVAL-FSM01M1 has an analog-to-digital converter it lacks helpful diagnostic triggers for my application of load detection and I will opt for oscilloscope measurements anyway which is more convenient and performs basically equivalent function. With this new design, I will use the IPS1025H high-side switch from STMicroelectronics which provides a fast demagnetization of inductive loads and smart driving of capacitive loads with tweakable current limitation. What is more important is that the smart driving function has a dedicated diagnostic pin to report when it becomes active and the demagnetization function alters the way an inductive load is driven which could be taken advantage of with a custom sensing circuit. Both of these signals can prove useful for my analysis. In summary, the things I want from this design are

i. Compatibility with NUCLEO-F401RE and NUCLEO-G431RB [38], [39] micro-controller boards that are readily available to me through Arduino UNO expansion connectors to take advantage of micro-controller pins to control switching and process diagnostic events and for power pins to the digital side of my board.
ii. Compatibility to be used in conjunction with STEVAL-FSM01M1 if needed
iii. Compatibility with standard 24V DC
iv. Semi-blocking of power with diodes and transil diodes from analog ground to help protect from over-voltage spikes and reverse polarity voltage
v. Complete isolation of digital ground to ideally avoid signal interference or damage from the power side to get to the micro-controller board
vi. Sensing of engagement of demagnetization function of IPS1025H switch
vii. Easy access to signal probing with the inclusion of test points and connectors for quick connection of loads, supply, power ground, and protective earth

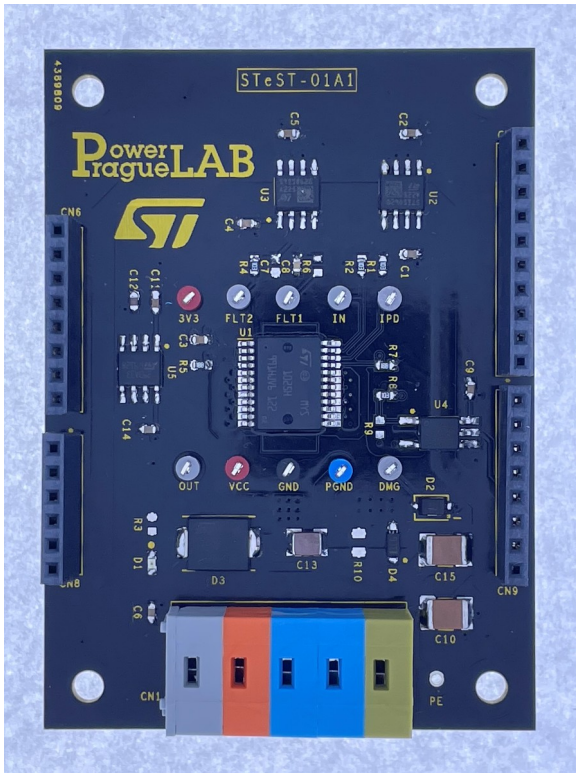

FIGURE 5: FINISHED EVALUATION BOARD

4.1 Schematic and components

4.1.1 Load switch

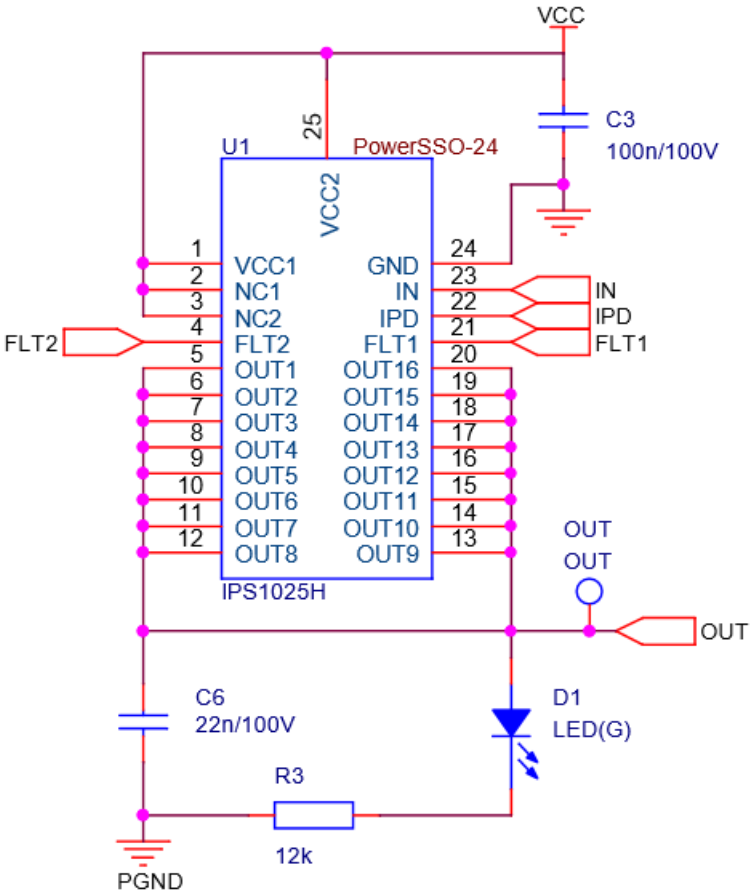

FIGURE 6: IPS1025H SWITCH IN THE DESIGN

TAB. 2: DESCRIPTION OF IPS1025H FUNCTIONS

Pin	Function
IN	Controls the switch state (open, closed)
OUTx	Output for powering load
IPD	Tweaks current limitation for capacitive loads with either high or low threshold or a combination of the two
FLT1	Thermal shutdown diagnostic pin. A current source that becomes active when thermal limitation is engaged.
FLT2	Overload diagnostic pin. A current source becomes active when the current limitation is engaged.

Surrounding capacitors have a blocking function for power delivery and single a LED is used to signal an active output stage. More detailed information about the IPS1025H switch is in its datasheet. [40]

4.1.2 Demagnetization sensing design

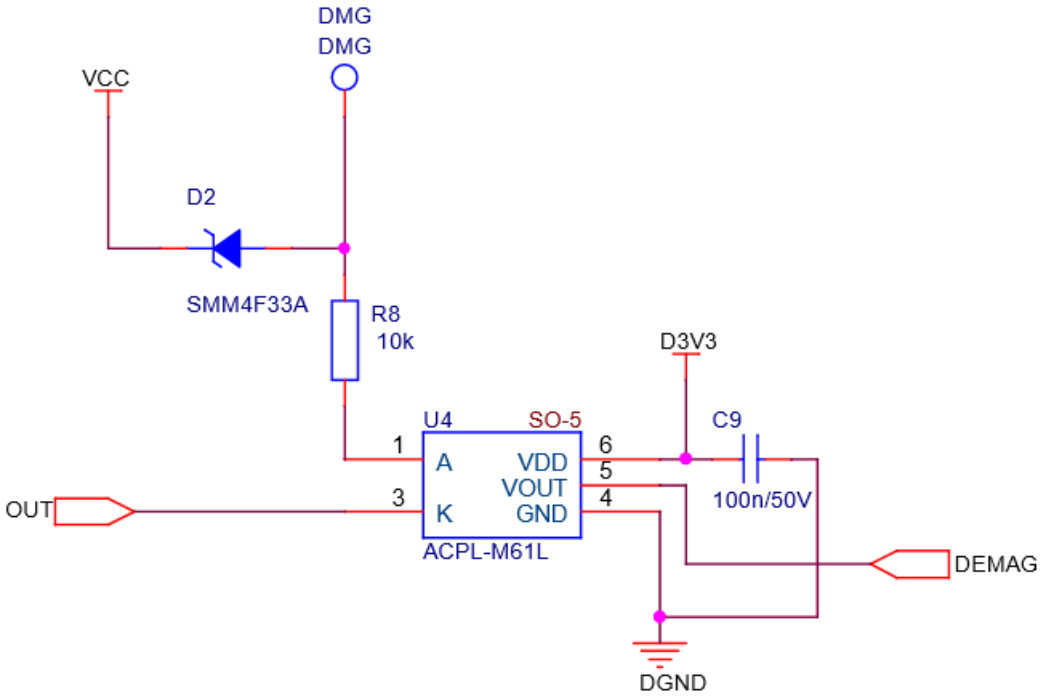

FIGURE 7: SCHEMATIC OF DEMAGNETIZATION SENSING DESIGN

TAB. 3: FUNCTIONALITY OF COMPONENTS IN THE DEMAGNETIZATION SENSING DESIGN

Component	Function
SMM4F33A	Transil diode is used as a trigger for demagnetization events [41]
ACPL-M61L	Digital optocoupler for isolation and digital signaling of triggered demagnetization event [42]
Passive components	Blocking for power and correct biasing of optocoupler

This custom circuit design in Figure 7 was devised with the help of consultation by a senior engineer in the STMicroelectronics laboratory [43]. The function of this circuit becomes clear with the introduction of the working principle of the demagnetization process used by the IPS1025H switch.

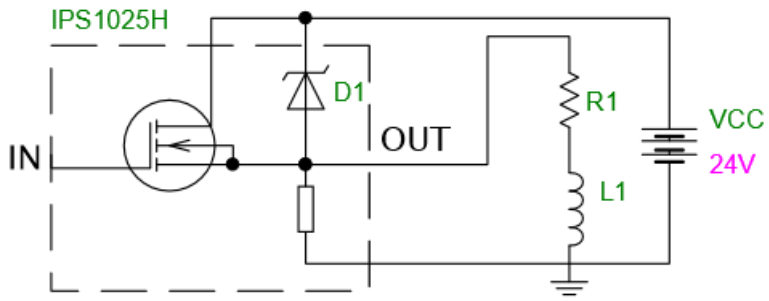

FIGURE 8: DIAGRAM OF THE WORKING PRINCIPLE OF DEMAGNETIZATION

The process of demagnetization can be explained with the help of the principal diagram in Figure 8. There are two distinct stages to this.

i. Gate voltage from the IN pin falls and the output transistor starts to close which causes a change in current in the inductor which causes voltage to be induced in accordance with formerly flowing current direction.
ii. The voltage at the OUT net becomes negative enough that a demagnetization clamp inside the switch breaks down and starts to conduct current which helps faster demagnetization of the inductor. Current flows until all energy is dissipated inside the switch and load resistance.

These facts lead to the creation of the demagnetization sensing design in Figure 7 which mimics the behavior of the internal clamp of the IPS1025H switch using a voltage clamping diode connected between the 24V supply and output of the switch. Both clamping elements however need to be activated at the same time and only if the internal clamp is active. Therefore it is important when choosing components to pay attention to the correct rating of the transil diode and optocoupler.

TAB. 4: RELEVANT COMPONENT RATINGS FOR CORRECT DEMAGNETIZATION SENSING

Component	Conditions
IPS1025H	After demagnetization is triggered the output voltage V_{DEMAG} of the switch is in the range from V_{CC}-76V to V_{CC}-68V [40]
SMM4F33A	Breakdown voltage V_{BR} in range from 37.1V to 41V, standoff voltage V_{RM} of 33V at 0.2μA and 25°C [41]
ACPL-M61L	Recommended operational current I_{FH} in the range from 1.6mA to 6mA, Active forward voltage V_F approx. 1V, Forward current in off-state I_{FL} up to 250μA [42]

To properly tune the sensing circuit first it is necessary to correctly rate the transil diode as the optocoupler rating will be dependent on it. After consultation with the senior engineer [43] we decided that 20% of supply voltage fluctuation will be acceptable for this application and the following conditions must be satisfied.

$$\begin{gathered} V_{CLAMP(min)} = V_{CC} - V_{DEMAG(max)} = V_{CC} - (V_{CC} - 68\,V) = 68\,V,\ V_{CC} = 24\,V \\ V_{CC(max)} = 1.2\,V_{CC} = 1.2 \cdot 24\,V = 28.8\,V \\ \Rightarrow V_{CC(max)} < V_{RM} \wedge V_{BR(max)} < V_{CLAMP(min)} \\ \Rightarrow V_{RM} > 28.8\,V \wedge V_{BR(max)} < 68\,V \end{gathered} \tag{11}$$

First, I need to make sure that the demagnetization sensing circuit activates if and only if there is demagnetizing voltage between the supply voltage and switch output within an IPS1025H specification as shown in tab. 4. We agreed on using transil diode model SMM4F33A (D2) available to our laboratory which has a standoff voltage above the maximum supply voltage which ensures that the diode will not conduct when it is not desirable. At the same time, the maximum breakdown voltage is lower than the minimum clamping voltage of the IPS1025H demagnetization. Concrete values are shown in (11) another factor in choosing this diode was its small package that does not waste extra space in the board design.

$$\begin{gathered} V_F = 1\,V,\ V_{BR(max)} = 41\,V \\ V_{bias(min)} = V_{CLAMP(min)} - V_{BR(max)} - V_F = 68\,V - 41\,V - 1\,V = 26\,V \end{gathered} \tag{12}$$

$$V_{BR(min)}=37.1\,V,\ V_{CLAMP(max)}=V_{CC}-V_{DEMAG(min)}=V_{CC}-(V_{CC}-76\,V)=76\,V$$
$$V_{bias(max)}=V_{CLAMP(max)}-V_{BR(min)}-V_F=76\,V-37.1\,V-1\,V=37.9\,V \quad (12)$$
$$V_{bias}=\frac{V_{bias(min)}+V_{bias(max)}}{2}=\frac{26\,V+37.9\,V}{2}=31.95\,V$$

$$I_{FH(min)}=1.6\,mA,\ I_{FH(max)}=6\,mA$$
$$I_{bias}=\frac{I_{FH(min)}+I_{FH(max)}}{2}=\frac{1.6\,mA+6\,mA}{2}=3.8\,mA \quad (13)$$

$$R_{bias}=\frac{V_{bias}}{I_{bias}}=\frac{31.95\,V}{0.0038\,A}\approx 8408\,\Omega \quad (14)$$

The second step is to choose an optocoupler here I decided to use any compact single-channel digital and push-pull output configuration. I settled on an ACPL-M61L optocoupler (U4) which I proceeded to bias according to the recommended operational current as shown in tab. 4. I biased the optocoupler by computing the bias resistance in the middle of possible voltage (12) and current (13) ranges for the optocoupler as a basis for deciding the final biasing resistance of the optocoupler. The resulting mean biasing resistance is 8408Ω (14). Here I decided to use a 10kΩ resistor (R8) as it still provides the optocoupler with a current within the recommended specification and avoids ordering redundant resistor values which I will not reuse elsewhere in the design.

4.1.3 Power and digital interfaces

To make this design compatible with digital control by NUCLEO-F401RE and NUCLEO-G431RB I again with input from the senior engineer [43] used a model of digital isolator STISO620 [44] (U2, U3) to route control and diagnostic signals from IPS1025H across an isolation gap and their schematic can be viewed in Figure B.1. Each isolator has two channels which nicely matches with the IPS1025H pins which are two diagnostic outputs FLT1 and FLT2 and two control inputs IN and IPD. As mentioned in tab. 2 the FLT1 and FLT2 two pins are current sources and need to be loaded for properly correct operation of the switch. From experience at the laboratory 1.2kΩ resistors (R5, R7) are optimal for this purpose in conjunction with other passive components placed according to good electronic design practices e. g. filtration and power blocking.

The physical connectors for digital electrical connection are done by Arduino UNO (CN5,6,8,9) compatible layout of header connectors and power electrical connection is done with WAGO (CN1) connectors with quick release. Both can be seen in the finished product in Figure 5. Schematic materials for them are available in Figure B.2.

The last schematic section Figure B.3 is for the interface between the power supply and inner power section of the board. Here I used two high-voltage capacitors (C10, C15) to create a net for a protective earth conductor. These capacitors are mainly for electromagnetic compatibility validations. Surge electrical protection is realized with bidirectional transil diode (D3) SM15T36CA [45] bidirectional transil diode that clamps voltage within admissible range to protect inner electronics. The second STPS1L60 [46] diode (D4) implements reverse polarity protection. Since the isolators need to be supplied voltage of 3.3V I have included the low drop-out voltage regulator LM2931 (U5) [47]. Since these parts serve as blocking for power to the whole board I opted for a combination of large and small capacitances.

4.2 Layout, assembly, and testing

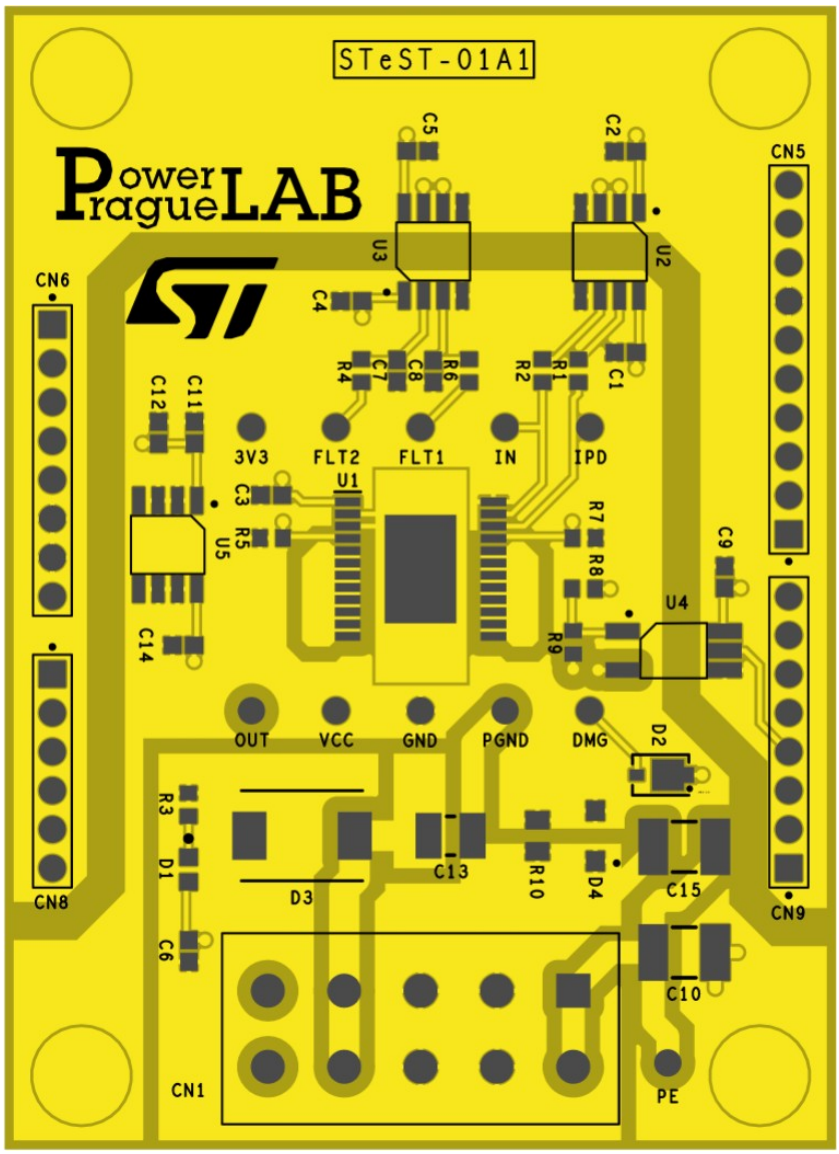

FIGURE 9: TOP LAYER LAYOUT WITH SILKSCREEN AND SOLDER MASK

Making the layout of the board was a straightforward process of designing pad stacks, package symbols, and combining everything on the board. There was not much issues since I had 4 layers to work with and a lot of space. Components related to the same functional blocks were placed in proximity to each other. During routing process I was following the common PCB design guidelines (minimizing surface of current loops, minimizing length of conductive traces, etc. Margins for pad stacks and spacing between components were kept larger since the assembly and necessary modifications would be made by hand without keeping the traces too long. The rest of the layout can be found in the Appendix from Figure B.4 to Figure B.7, parts in tab. B.1.

After the reception of manufactured boards and their assembly by hand, there was a brief period of testing and debugging of a few sections of the circuit concerning soldering issues and tweaks to the output capacitor at the output of the low drop-out regulator for stabilization. After the board worked as intended verified by measurement. I will proceed to the measurements now.

5 Measurements and methods

Measurements will be the next important part of this work and will be instrumental to answering the posed issue of how to detect and determine the parameters of connected loads. This work is not focused on getting the most accurate results as long as they are accurate enough not to be misleading far more important are principles and methods. There are four main points to these measurements.

i. Ensure and verify the correct function of the board
ii. Check the results of measurements against the theory laid out in Chapter 2.2
iii. Study the behavior of signals of different loads to come up with solutions to the detection of tested loads and their parameters.
iv. Saved measured waveform data is used to demonstrate the calculation results of different methods.

For this purpose, the senior engineer [43] has given me a choice between some common actuators used in industrial automation which were at the time available in our laboratory. These included in terms of inductive loads solenoid coil and contactor or electromagnetic motor brake. In terms of capacitive loads, I was free to design my own load since there is not much in terms of common purely capacitive actuators. The last type of load I should study would be an incandescent light bulb.

This section of the work is structured as a chronological journal recording all experimentation and introduces ideas as they are formed keeping with the chronological order. A summary of the results is in Chapter 7.

5.1 Resistive and inductive load

I have decided to group the two types of loads since they share a lot in common. Simply said it is possible to look at a resistor as an inductive load where the time constant of current tends to zero.

5.1.1 Resistor

Measurements on resistive load with constant resistance should be straightforward and are included here just for the sake of completeness of documentation in continuation to the chapter laying out the theoretical background. The obligatory measurements can be found in Figure C.1 and Figure C.2. Both measurements adhere to the theoretical expectations voltage and current step-up and down at virtually the same time. This measurement shows us that the switching functions correctly.

TAB. 5: MEASURED PARAMETERS OF 47Ω RESISTOR ON VOLTAGE STEP UP/DOWN

V_{CC} (V)	24.2
V_1 (V)	24
I_1 (mA)	494
R_1 (Ω)	48.58

Measured parameters when the resistive load is switched are displayed in tab. 5. For all upcoming calculations the formula for steady-state resistance will be (15).

$$R_1 = \frac{V_1}{I_1} \qquad (15)$$

5.1.2 Solenoid coil

Measuring an inductive load provides more interesting results. The first measurements with the solenoid coil prove to adhere to the theoretical expectations. When the output voltage is switched on the current through the coil follows an exponential growth until it reaches the steady state which is defined by the resistance of the coil. The described phenomenon can be observed in Figure C.3. I measured steady-state values of signals and calculated peak power and total energy to fully magnetize the coil.

TAB. 6: MEASURED PARAMETERS OF 1.2H, 14Ω SOLENOID ON VOLTAGE STEP UP

V_{CC} (V)	24.4
V_1 (V)	24
I_1 (A)	1.78
R_1 (Ω)	13.48
P_{INFLUX} (W)	41.27
E_{INFLUX} (J)	3.91

Now I have quantities that characterize the transient event. The computed quantities were calculated inside an oscilloscope with mathematical formulas. For all upcoming measurements, the formula for power and energy when the inductive load gets switched on will be (16) and (17) respectively.

$$P_{INFLUX}(t) = v_1(t) \cdot (I_1 - i(t)) \quad (16)$$

$$E_{INFLUX}(t) = \int_0^T P_{INFLUX}(t)\,dt = \int_0^T v_1(t) \cdot (I_1 - i(t))\,dt \quad (17)$$

These are just general measured parameters of the transpiring event so I can get acquainted with it and maybe use them later to my advantage. Remembering the theory from the beginning the most characteristic and visually striking difference when comparing different loads is how they differ in terms of interaction between voltage and current signals that power them and how they change in relation to each other.

Since I have the raw data of each characteristic oscilloscope measurement I can verify if the introductory theory is actually reflected in the dataset. It definitely looks like exponential growth with a steady state in the oscillogram but we can perform regression to make sure that it is really true. For this, I have used a Python fitting tool [48] which I found online, and attempted to fit a function to the dataset with quite good results.

$$y = b + (a - b) \cdot e^{-cx^d}, b = I_1, a = I_0, c = \frac{R_1}{L_1}, d \to 1 \quad (18)$$

TAB. 7: COMPARISON BETWEEN MEASURED AND REGRESSION FIT SOLENOID PARAMETERS

Parameters	Expected value	Fitted value
a (A)	0	0.012
b (A)	1.780	1.767
c (s^{-1})	11.233*	10.666
d (-)	1	0.992
R^2 (-)	1	0.998

* Inductance measured by a scale on the solenoid

We can see that by fitting a function to the data we get quite close to the measured and set parameters. This can be used to build a model of powered load if we have enough computational power at hand. These fitted parameters allow us to compute the relevant inductance in (19).

$$c=\frac{R_1}{L_1}\Rightarrow L_1=\frac{R_1}{c}\approx\frac{13.48\,\Omega}{10.67\,s^{-1}}\approx 1.26\,H \quad (19)$$

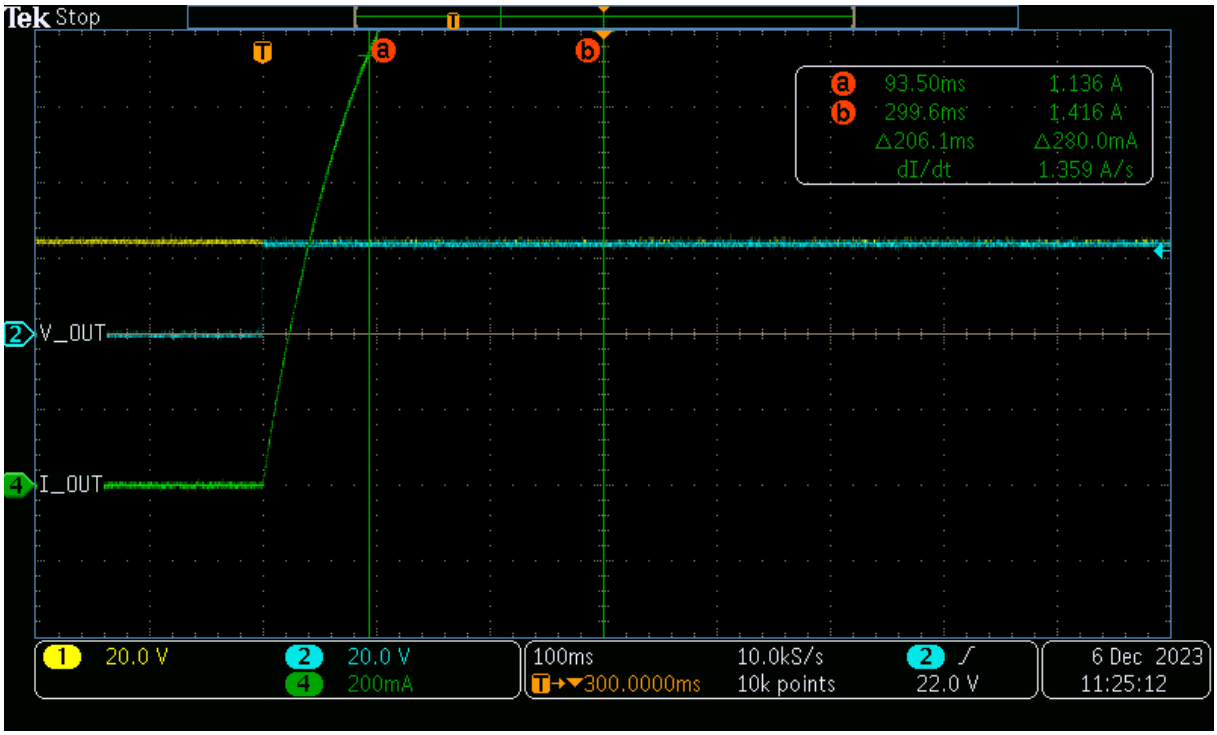

FIGURE 10: MEASUREMENT OF TIME CONSTANT AT THE KNOWN CURRENT EXPONENTIAL LEVEL IN THE INDUCTIVE LOAD

Another possible approach is to do a simple readout of a time constant at the corresponding exponential level of the current waveform shown in Figure 10.

It can be derived by taking differential geometrically which is a generally known process of taking the derivative at the origin of transient step response and finding the time constant of inductive load from interception with time axis. The other way is to modify equation (5) for this purpose and solve for the time when the time constant is reached.

$$t=\tau:\ \ i(\tau)=I_1-I_1\cdot e^{-1}=I_1\cdot\left(1-\frac{1}{e}\right)\approx 1.8\,A\cdot 0.632=1.14\,A \quad (20)$$

Now I use the calculated current value from (20) for measurement of the time constant from waveform in Figure 10 at cursor a.

$$\tau=93.5\,ms\Rightarrow L_1=\tau\cdot R_1\approx 0.0935\,s\cdot 13.56\,\Omega=1.27\,H \quad (21)$$

Comparing it to the results of the regression fitted function it gets quite close in terms of computed inductance. Now to get back to studying how the waveform evolves in time and quantify it. After trying to compute different parameters about the waveform I settled on a measure of areas.

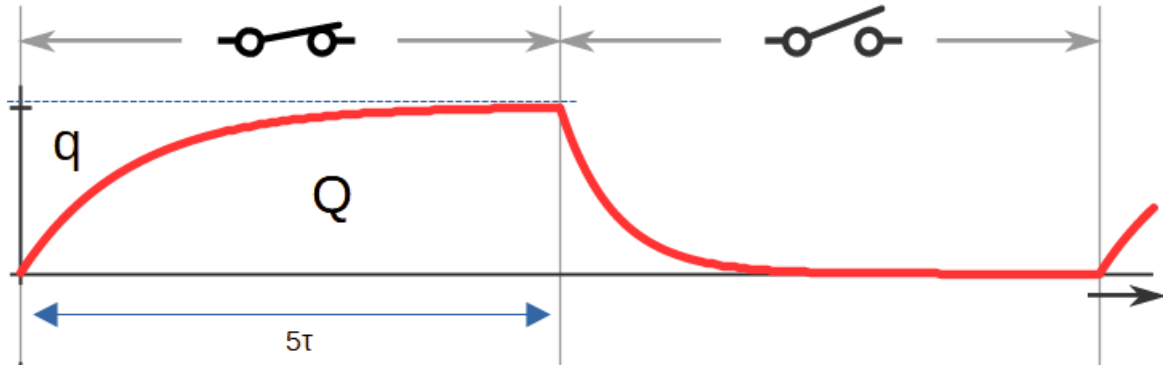

FIGURE 11: DETECTION AND DETERMINATION PRINCIPLE USING THE AREA UNDER THE TRANSIENT

Figure 11 based on [49] is the setup for the detection method of the inductive load when it is switched on. I will use ratio of actual transient charge to a charge window formed by actual transient current and time. This idea is put into mathematical formula (22).

$$Q=\int_0^T i(t)\,dt=\int_0^T I_1-I_1\cdot e^{(-t/\tau)}\,dt=T\cdot I_1+\tau\cdot I_1\cdot\left(e^{(-T/\tau)}-1\right)$$
$$Q+q=T\cdot I_1 \qquad (22)$$
$$\sigma=\frac{Q}{Q+q}=\frac{T\cdot I_1+\tau\cdot I_1\cdot\left(e^{(-T/\tau)}-1\right)}{T\cdot I_1}=1+\frac{\tau}{T}\left(e^{(-T/\tau)}-1\right)$$

Now I will compute the defined ratio for the steady state.

$$T=5\tau:\sigma=1+\frac{\tau}{5\tau}\left(e^{(-5\tau/\tau)}-1\right)\approx 0.8013\Rightarrow T\geq 5\tau\Rightarrow\sigma\geq 0.8013 \qquad (23)$$

Using the computed condition in (23) will make it easy to detect both steady state and time constant. If the size of the time constant is diminutive than the load is mostly resistive. This principle can be used for other inductive loads and even adapted for capacitive loads if the analyzed signal follows closely the exponential characteristic. When this condition is triggered it is also possible to compute inductance since it triggers when steady state is reached we have the steady state resistance available for computation as well as the time constant. For the measured waveform this gives (24).

$$L_1=\tau\cdot R_1\approx 0.09\,s\cdot 13.64\,\Omega\approx 1.23\,H \qquad (24)$$

The concept of ratio of areas under the curve with the one under the horizontal coordinate of the actual data point can be used as a part of a more general detection method for steady state detection where periodically the ratio calculation starting point is re-anchored on the curve and the ratio should tend to one as steady state is reached. More about this method in Results chapter.

When switching the output voltage off in this case there is not a standard transient decay but a demagnetization function of the IPS1025H is engaged which results in considerably different response. This event is depicted in Figure C.4 with following basic measured parameters.

TAB. 8: MEASURED PARAMETERS OF 1.2H, 14Ω SOLENOID ON VOLTAGE STEP DOWN

V_{CC} (V)	24.8
V_1 (V)	24
V_{DEMAG} (V)	-47.2
I_1 (A)	1.78
R_1 (Ω)	13.48
P_{SWITCH} (W)	128.2
E_{SWITCH} (J)	2.24
P_{DEMAG} (W)	81.98
E_{DEMAG} (J)	1.46
T_{DEMAG} (ms)	37.8

Some quick observations of tab. 8 show that compared to when voltage is switched on this time the process is much more power dense and we have two power emitters the high side switch with its demagnetizing feature and the solenoid. Combined peak power is approximately 210W compared to 41W. The energy gets to be distributed between those and stays virtually same at combined 3.7J compared to the previous event. The added custom detection circuit generates pulse which should ideally have duration of demagnetization process. Here it is 37.8ms which is about about one magnitude shorter compared to when steady state is reached on voltage step up.

Measuring energy is useful as it is another way the inductance can be calculated. When comparing energies of the two events with analogous formulas for an inductive load to those from chapter 2.2.2. When the solenoid gets switched on we have formula (25).

$$E_{INFLUX} = \int_0^{T_{STEADY}} v_1(t)\cdot i(t)\,dt = V_1 \int_0^{T_{STEADY}} I_1 - I_{DECAY}\left(1-e^{(-t/\tau)}\right)dt,$$
$$I_{DECAY} = I_1 \qquad (25)$$
$$\Rightarrow E_{INFLUX} = V_1\cdot I_1 \int_0^{T_{STEADY}} e^{(-t/\tau)}\,dt = V_1\cdot I_1\cdot\left(\tau-\tau\cdot e^{(-T_{STEADY}/\tau)}\right)$$

Now I solve for time condition when electrical transient of a first order circuit reaches its steady state.

$$T_{STEADY}\rightarrow\infty:\ \tau = \frac{E_{INFLUX}}{V_1\cdot I_1} \Rightarrow \tau = \frac{3.91\,J}{24\,V\cdot 1.78\,A} \approx 92\,ms \qquad (26)$$
$$\Rightarrow L_1 = \tau\cdot R_1 = 0.092\,s\cdot 13.48\,\Omega \approx 1.23\,H$$

Now for the comparison when the solenoid is switched off an analogous derivation process to that of (25) can be used. And can be found in a ST design manual UM1922 for high side switches.

(27)

$$I_{DECAY}=I_1+I_{DEMAG},I_{DEMAG}=\frac{V_{DEMAG}}{R_1}$$

$$\tau=\frac{R_1\cdot E_{DEMAG}}{|V_{DEMAG}|\cdot\left(V_1-|V_{DEMAG}|\cdot\ln\left(\frac{|V_{DEMAG}|+V_1}{|V_{DEMAG}|}\right)\right)}\approx\frac{13.48\,\Omega\cdot 1.46\,J}{47.2\,V\cdot\left(24\,V-47.2\,V\cdot\ln\left(\frac{47.2V+24\,V}{47.2\,V}\right)\right)}\approx 91\,ms$$

$$\Rightarrow L_1=\tau\cdot R_1\approx 0.091\,s\cdot 13.48\,\Omega\approx 1.22\,H$$

Formulas (26) and(27) show that using energy as a basis for inductance calculation can be beneficial both on voltage step up and step down. One big advantage of calculating inductance from energy is that it does utilize the whole waveform for computation and diminishes chance for possible single point of failure which could be problem for the direct time constant readout and is easier to compute than performing regression fit while getting still quite close to the true value of inductance (19).

5.1.3 Electromagnetic motor brake

The solenoid was purely electromagnetic element. This next load has a mechanical actuation mechanism set in motion by magnetic force. As such the geometric relations between the parts inside change on actuation. It is to be expected that the magnetic field will change during this process and it is confirmed by Figure C.5. However since I only use purely electrical models I will use the energy model for purely inductive load. It is possible to extract following parameters from the measurement.

TAB. 9: MEASURED PARAMETERS OF ELECTROMAGNETIC BRAKE ON VOLTAGE STEP UP

V_{CC} (V)	24
V_1 (V)	23.9
I_1 (A)	2.38
R_1 (Ω)	10.04
P_{INFLUX} (W)	55.2
E_{INFLUX} (J)	2.27

Like before (26) I will compute the time constant and inductance from energy spent to energize the magnetic field of electromagnetic brake using data from tab. 9.

$$\tau=\frac{E_{INFLUX}}{V_1\cdot I_1}\Rightarrow\tau=\frac{2.27\,J}{23.9\,V\cdot 2.38\,A}\approx 40\,ms\Rightarrow L_1=\tau\cdot R_1=0.04\,s\cdot 10.04\,\Omega\approx 0.4\,H \qquad (28)$$

Next comes the switch off of the brake. The transient event is shown in Figure C.6. Extracted characteristic parameters are in tab. 10.

TAB. 10: MEASURED PARAMETERS OF ELECTROMAGNETIC BRAKE ON VOLTAGE STEP DOWN

V_{CC} (V)	24.8
V_1 (V)	24
V_{DEMAG} (V)	-46.4
I_1 (A)	2.38
R_1 (Ω)	10.08
P_{DEMAG} (W)	107
E_{DEMAG} (J)	0.31
T_{DEMAG} (ms)	12

Thing to note is that the demagnetization voltage recovery is slower when switching the brake off which leads to incorrect time duration measurement by demagnetization detection pulse.

It will be interesting to compare the inductance of the electromagnetic motor brake between the switch on and inductance. It is important to note that the inductance most probably changes during actuation. So the inductance here is more of an equivalent inductance of the whole transient event. We can use the formula from(27).

(29)

$$\tau = \frac{R_1 \cdot E_{DEMAG}}{|V_{DEMAG}| \cdot \left(V_1 - |V_{DEMAG}| \cdot \ln\left(\frac{|V_{DEMAG}| + V_1}{|V_{DEMAG}|} \right) \right)} \approx \frac{10.08\,\Omega \cdot 0.31\,J}{46.4\,V \cdot \left(24\,V - 46.4\,V \cdot \ln\left(\frac{46.4\,V + 24\,V}{46.4\,V} \right) \right)} \approx 14\,ms$$

$$\Rightarrow L_1 = \tau \cdot R_1 \approx 0.014\,s \cdot 10.08\,\Omega \approx 0.15\,H$$

It is apparent that the internal inductance of the electromagnetic motor brake changes with actuation. One explanation could be that a ferromagnetic material gets pulled into the winding of the actuation mechanism when switched on and gets mechanically repelled when switched off.

5.2 Capacitive load and incandescent load

I have decided to group the two types of loads together since they share a lot in common when switched on from the measurements. Simply said it is possible to look at a resistor as an capacitive load where time constant of current and voltage tends to zero.

5.2.1 Capacitive load

Since there are no widespread actuators with capacitive driving forces other than a precision specialty drives in niche applications. I will consider the capacitive load as an auxiliary part to all types of industrial devices like electronics to power actuators, sensing devices and industrial electronics in general and other inherent capacitances used in concrete applications.

To enter this topic I started with a measurement of a transient when a capacitive load gets switched on which is shown in Figure C.7 and shows the and shows rough traits of the simulation in Figure A.3 even if current limitation occurs. Current steps up at the same time as voltage with discontinuity and a peak at the origin of the transient and then decays converging to steady state current or current decays to zero when

switched off. Measured parameters are shown in tab. 11 formulas for computed parameters are listed in (30). In this case overload detection of IPS1025H also has a delay and as such I can not use it to time the true duration of the overload.

TAB. 11: MEASURED PARAMETERS OF 100MF LOAD ON VOLTAGE STEP UP

V_{CC} (V)	24.3
V_1 (V)	24.2
I_1 (A)	0.5
R_1 (Ω)	48.4
P_{INRUSH} (W)	48.5
E_{INRUSH} (mJ)	35.94
$T_{OVERLOAD}$ (µs)	395

$$P_{INRUSH}(t)=v_1(t)\cdot(i(t)-I_1)$$
$$E_{INRUSH}(t)=\int_0^{T_{STEADY}} P_{INRUSH}(t)dt=\int_0^{T_{STEADY}} v_1(t)\cdot(i(t)-I_1)dt \qquad (30)$$

The approach to calculation of capacitance will be different compared to inductive load. In this case the formula (8) from theoretical introduction does not fit this scenario since both voltage and current are too deformed by the current limitation. However there is one advantage in this situation. In the case of inductance we could not simply use the equation for its energy since it had a series resistance. Here I can use basic energy equation since the switched voltage falls directly across the capacitor.

$$E_{INRUSH}=\frac{1}{2}C_1\cdot V_1^2\Rightarrow C_1=\frac{2E_{INRUSH}}{V_1^2}\approx\frac{2\cdot 0.036\,J}{24.2^2\,V^2}\approx 123\,\mu F \qquad (31)$$

A diligent reader might argue that formula (30) is not entirely exact and that is true. However the slowly rising voltage when the switch is in current limitation biases the current difference towards the steady state. Just for comparison I tried multiple ways to compute the energy numerically from waveform data.

$$E_{INRUSH}=E-E_R=\int_0^{T_{STEADY}} v_1(t)\cdot i(t)-\frac{v_1^2(t)}{R_1}dt\approx 0.053\,J-0.015\,J=0.038\,J$$
$$\Rightarrow C_1=\frac{2E_{INRUSH}}{V_1^2}\approx\frac{2\cdot 0.038\,J}{24.2^2\,V^2}\approx 131\,\mu F \qquad (32)$$

$$E_{INRUSH}=E-P_{STEADY}\cdot T_{STEADY}=\int_0^{T_{STEADY}} v_1(t)\cdot i(t)\,dt-V_1\cdot I_1\cdot T_{STEADY}\approx 0.053\,J-0.019\,J=$$
$$=0.034\,J$$
$$\Rightarrow C_1=\frac{2E_{INRUSH}}{V_1^2}\approx\frac{2\cdot 0.034\,J}{24.2^2\,V^2}\approx 114\,\mu F \qquad (33)$$

The results from two calculations of capacitance in (32) and (33) seem all somewhat close. The second calculation has the benefit that it works without knowledge of the steady state resistance as such it can be used for determining a capacitance which has to have the resistance determined on the first switch on. It is apparent that the result of previous calculation (31) lies in the middle of the two.

When capacitive load is switched off the capacitor discharging through a resistor causes the voltage at the output of the switch to decay slowly this is shown in Figure C.8. The basic parameters are shown in tab. 12.

TAB. 12: MEASURED PARAMETERS OF 100MF LOAD ON VOLTAGE STEP DOWN

V_{cc} (V)	24.2
V_1 (V)	24
I_1 (mA)	496
R_1 (Ω)	48.39

We can fit a function with regression to this decaying waveform in form of formula (34).

$$y = a \cdot e^{-bx} \qquad (34)$$

TAB. 13: COMPARISON BETWEEN MEASURED AND REGRESSION FIT CAPACITANCE PARAMETERS

Parameters	Expected value	Fitted value
a (V)	24	24
b (s^{-1})	208.33	202.94

The resulting regression fitted parameters are shown in tab. 13. From these I can compute the capacitance with formula (35).

$$\tau = \frac{1}{b} = \frac{1}{202.94\, s^{-1}} \approx 4.93\, ms \Rightarrow C_1 = \frac{\tau}{R_1} = \frac{0.00493\, s}{48.39\, \Omega} \approx 102\, \mu F \quad (35)$$

Another way of computing the capacitance when the capacitive load is switched off is with the help off the governing equation of the transient which can be derived from (8) in 2.2.3 considering switch off as open circuit at R_1.

$$R_1 \to \infty : v_1(t) = V_0 \cdot e^{(-t/\tau)} \Rightarrow \tau = \frac{t}{\ln \frac{V_0}{v_1(t)}} \qquad (36)$$

Using the formula (36) for a waveform data has a few caveats since the formula is not defined at the edges of a transient waveform however if we for example average such computed time constants in voltage range from 21.6V to 2.4V in other words middle 80% interval of voltage range. This gets us result in (37).

$$\bar{\tau} \approx 0.0049\, s \Rightarrow C_1 = \frac{\tau}{R_1} \approx \frac{0.0049\, s}{48.39\, \Omega} \approx 101\, \mu F \qquad (37)$$

This principle is not specific to the capacitive load and can be used for any load that exhibits characteristic exponential transient behavior.

5.2.2 Incandescent light bulb

Measured incandescent light bulbs also trigger current limitation and the way they switch on is very similar to a capacitive load the exact behavior is shown by measurement in Figure C.9. The question is if I can differentiate these two reliably.

TAB. 14: MEASURED PARAMETERS OF 1A INCANDESCENT LIGHT BULB ON VOLTAGE STEP UP

V_{CC} (V)	24.3
V_1 (V)	24
I_1 (A)	1.12
R_1 (Ω)	21.43
P_{INRUSH} (W)	43.2
E_{INRUSH} (J)	1.25
$T_{OVERLOAD}$ (ms)	14.35

Basic measured parameters can be reviewed in tab. 14. Waveform parameters can be closely matched between incandescent light bulb and load put together according to schematic in Figure 3 as such equations for inrush power and energy can be reused from (30). I have tried to match the 1A incandescent light bulb to such a load which resulted in parameters in tab. 15.

TAB. 15: CAPACITIVE LOAD PARAMETERS MATCHED TO INCANDESCENT LOAD

R_0 (Ω)	1
R_1 (Ω)	20
C_1 (μF)	2070

This is the closest I could get the waveform of the two loads match with available passive components in the laboratory and the available range of the current probe. The comparisons can be reviewed in Figure C.10 and Figure C.11 with and without current limitation. From the measurements it seems that there is not much difference. The most standout differences are the peak in capacitive load when it is switched on and the slower decay in current in incandescent load. However the differences are so diminutive that I doubt I will be able to derive a reliable detection method from this. Instead I will focus on the difference when the incandescent load gets switched off.

Behavior of incandescent load when switched off can be reviewed in Figure C.12 and when compared to the Figure C.2 and Figure C.8 it is immediately apparent that the light bulb switches off like a regular resistor. For detection I will use notions laid out in Figure 11 and (22) to distinguish capacitive load from incandescent.

Starting from capacitive load with formula (8) the series resitor allows me to simulate switch off of the capacitive load.

$$R_0 \to \infty : v_{DECAY}(t) = v_1(t) = v_{RC}(t) = V_0 \cdot e^{(-t/\tau)} \Rightarrow v_{GROWTH}(t) = V_0 - v_{DECAY}(t) \quad (38)$$

$$\sigma = \frac{1}{T \cdot V_0} \int_0^T v_{GROWTH}(t)\, dt = \frac{T \cdot V_0 + \tau \cdot V_0 \cdot \left(e^{(-T/\tau)} - 1\right)}{T \cdot V_0} = 1 + \frac{\tau}{T}\left(e^{(-T/\tau)} - 1\right) \quad (39)$$

Here I converted the exponential decay to complementary growth (38) since both carry the same rate of change and used it to define the same relation as with the inductive case (39) which goes together with the same condition for time constant (23). Again a diminutive time constant means mostly incandescent load.

The only elementary parameter of incandescent load is its resistance which could be measured in different ways. One way is already included in tab. 14 with steady state resistance.

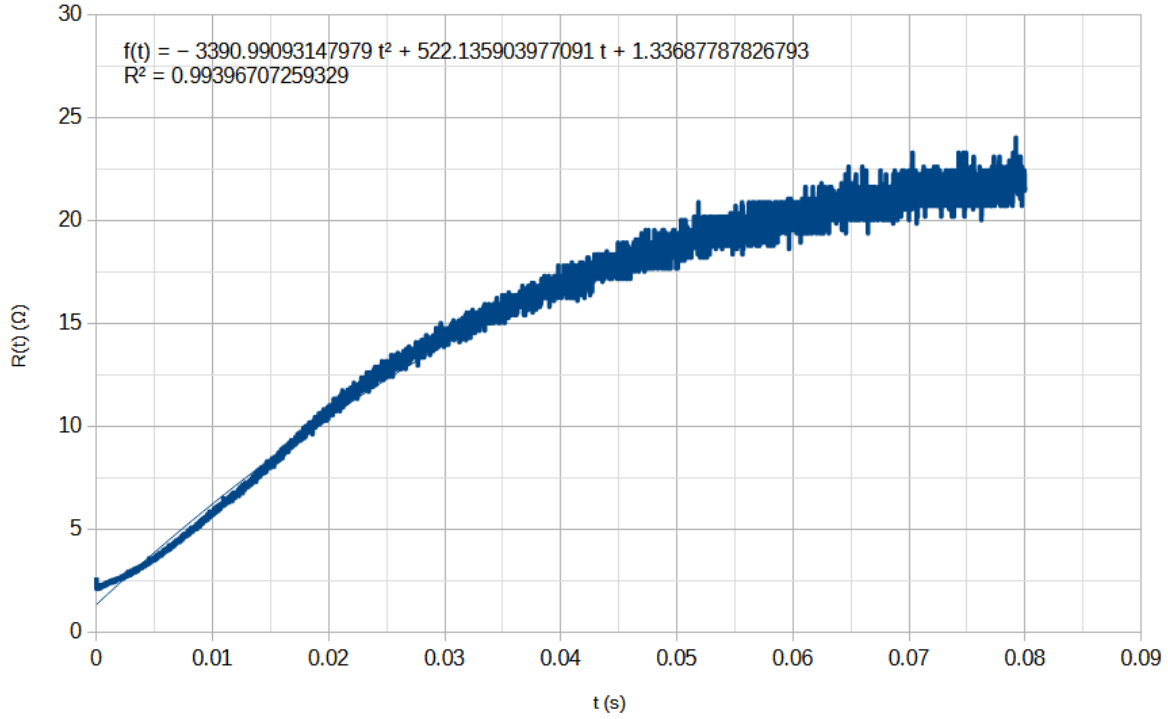

FIGURE 12: RESISTANCE OF INCANDESCENT FILAMENT

To familiarize myself with the resistance of incandescent filament I have plotted it against time for when it is switched on in Figure 12. It is closely related to a second degree polynomial function. However we can use the saved waveform data to calculate other resistance related parameters.

TAB. 16: OTHER POSSIBLE RESISTANCES OF INTEREST FOR INCANDESCENT LOAD

R_{COLD} (Ω)	2.1
$R_{EFFECTIVE}$ (Ω)	11.3

Cold resistance in tab. 16 is when the filament is at room temperature when it gets switched on and effective resistance is derived from root mean square values of current and voltage when the incandescent bulb is getting switched on. More formally put in formula (40).

$$R_{COLD} = \frac{V_1}{I_1} at\ \theta \approx 20\,°C$$
$$R_{EFFECTIVE} = \frac{\sqrt{\frac{1}{T_{STEADY}} \int_0^{T_{STEADY}} i^2(t)\,dt}}{\sqrt{\frac{1}{T_{STEADY}} \int_0^{T_{STEADY}} v_1^2(t)\,dt}} \qquad (40)$$

6 Algorithmic solutions

This chapter is the culmination of all previous endeavors so far from the design of functional measurement sample to the analysis of measured data and creation of methods and techniques for detection and determination of typical parameters of switched loads. All this acquired knowledge will now be used to put together an automatic algorithms which will decide what type of load is being switched and calculate its parameters. Each algorithm will be introduced by step by step description in natural language. Some of them will also include diagram or pseudocode if the algorithm is not trivial and can be described with it in a clear and compact way.

6.1 Detection algorithms

6.1.1 Electrical parameter detection algorithm

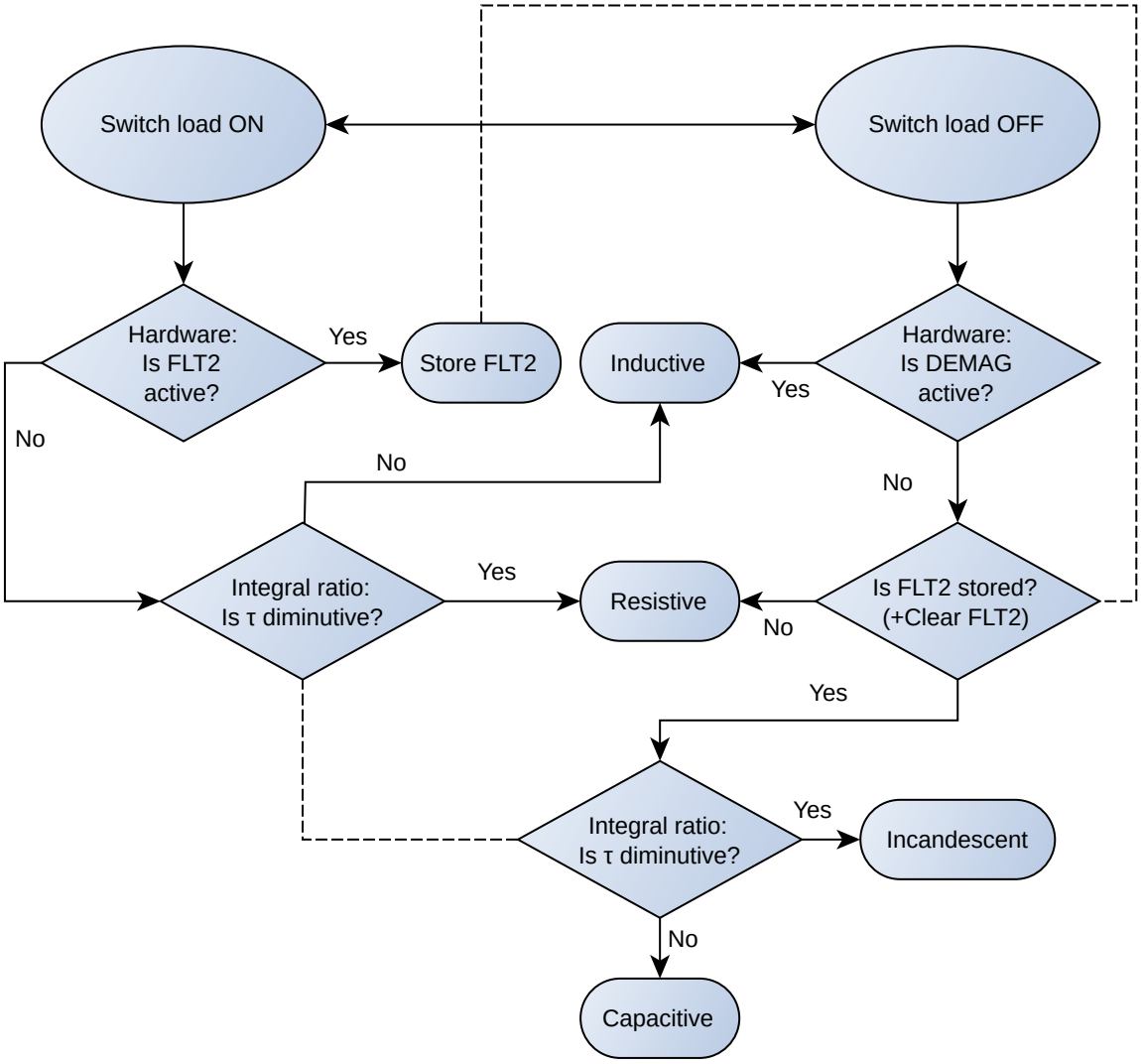

Figure 13: Decision algorithm diagram for detection method

For formative ideas behind this algorithm see 4.1.1, 4.1.2 especially Figure 11, (22), (23) in chapter 5.1.2 and (38), (39) in chapter 5.2.2.

1 Switch load on

1.1 If FLT2 pin gets activated set a flag carry over state of FLT2 pin activation and wait for switch off.

1.2 Otherwise use Integral ratio method for computation of the current time constant of the switched load and if it is diminutive e. g. less than application specific time constant threshold it is proclaimed resistive in the other case it is proclaimed inductive.

2 Switch load off

2.1 If DEMAG pin gets activated the switched load is proclaimed inductive

2.2 If FLT2 pin activation carry over flag state is set then use the Integral ratio method to compute the voltage time constant of the switched load and if it is diminutive e. g. less than application specific time constant threshold it is proclaimed incandescent in the other case it is proclaimed capacitive.

2.3 Otherwise the Integral ratio method is used to compute time constant of the switched load and if it is diminutive e. g. less than application specific time constant threshold it is proclaimed resistive in the other case it is proclaimed inductive.

We clearly have some redundancy in terms of Hardware and Integral ratio methods sharing a set of detection outcomes which is not necessary a bad thing and could be used to improve the correctness of detection. Algorithm for the Integral ratio method is described in following sections.

6.1.2 Steady state detection algorithm

```
import measurement // Measurement series
import timeout // Application timeout
import state // Application defined states and their levels

logic procedure steady_state_detection(
    input float area_ratio, /* Expresses how much area under exponential covers area under the max. amplitude. See (22), (23). */
    input float time_threshold, // Duration of a measured slice depends on apllication, but time constant can be a guiding parameter
    input float initial_amplitude // Steady state amplitude before switching
) do
    set float area_accumulator = 0 // Accumulator of elementary areas - Integral implementation
    set float time_accumulator = 0 // Accumulator of time
    set float max_amplitude = initial_amplitude // Max amplitude in a measured slice

    timeout.start();
    foreach (sample in measurement.samples) do

        if (timeout.is_expired) do
            output "Warning: calculation timed out."
            break
        end

        if (sample.amplitude > max_amplitude) do
            set max_amplitude = sample.amplitude
        end

        set time_accumulator += measurement.period
        set area_accumulator += sample.amplitude * measurement.period

        if (state.is_low(max_amplitude)) do
            timeout.reset()
            return True
        end else if (time_accumulator > time_threshold) do
            timeout.reset()
            set float ratio = area_accumulator/(max_amplitude * time_accumulator)

            return ratio >= area_ratio
        end
    end
end
```

FIGURE 14: PSEUDOCODE IMPLEMENTATION OF STEADY STATE DETECTION ALGORITHM
For formative ideas behind this algorithm see Figure 11, formulas (22) and (23) in chapter 5.1.2.

1 Define accumulator memory variables for area and time

2 Define an application threshold constant with value of ratio of areas between the one under the analyzed signal curve and the one under the horizontal coordinate of maximum amplitude

3 Define application constant for time threshold of each integral computation interval

4 Define variable for max amplitude

5 Sample data point with from analyzed signal add time between samples to the time accumulator and product sample amplitude and time between samples to the area accumulator

6 If actual sample amplitude is greater than the maximum amplitude overwrite reference amplitude with sample amplitude

7 If time accumulator is greater than time threshold then compute the ratio between the area accumulator and product of time accumulator and maximum amplitude. If the ratio is greater than ratio threshold from step 2 then proclaim that signal has reached a steady state. Otherwise zero out area, time accumulator and maximum amplitude and continue with step 5.

6.2 Determination algorithms

This section will introduce algorithms for determination methods using principles observed in Measurements and methods chapter. Diagrams for determination algorithms will be provided by a sequence of written instruction steps. Each method will start with set of limitations which need to be met and the method does not provide.

6.2.1 Trivial physical laws

Limitations: Knowledge that steady state has been reached

For formative ideas behind this algorithm see formula (15) in chapter 5.1.1

1. Sample single data point of current and voltage with when load is switched on
2. Compute steady state resistance in accordance with Ohm's law

6.2.2 Regression fit parameters

Limitations: Data follows exponential transient characteristic, available implementation of nonlinear regression fitting subprogram

For formative ideas behind this algorithm see formulas, (18), (19), (34), (35) and tab. 7, tab. 13 in chapter 5.1.2, 5.2.1

1. Sample single data points of current or voltage with converter and add their coordinates to arrays for amplitude and time between samples from the moment load is switched until steady state or application specific time is reached
2. Pass the arrays of data points to nonlinear regression fitting subprogram which finds the best fitting function
3. Use the regression fit parameters given by the fitted function to extract the time constant of the switched load

6.2.3 Time constant determination at known exponential level

Limitations: Data follows exponential transient characteristic, Known defined exponential level (here it is 63.2% when switched on and 36.8% when switched off), Knowledge of steady state amplitude

For formative ideas for this algorithm see Figure 10 and formulas (20) and (21) in chapter 5.1.2

1. Define two double element arrays one for time and one for amplitude
2. Define the known exponential level from known steady state amplitude e. g. 63.2% or 36.8% of steady state amplitude.
3. Sample two consecutive data points of analyzed voltage or current signal with converter and store them inside the arrays for amplitude and time.
4. If the known exponential level is within the bounds of the two stored amplitude values included take the average of time array values and proclaim it a time constant of the switched load.
5. Otherwise sample single data point and push it inside the arrays with pushing out of the oldest data point. Get back to step 4 and continue.

6.2.4 Integral ratio

Limitations: Data follows exponential transient characteristic

For formative ideas behind this algorithm see Figure 11 and formulas (22), (23), (24), (38), (39) in chapters 5.1.2, 5.2.2

1. Define reference time as a scaled time constant value (preferably 5 time constants which comes with the added benefit of steady state detection like I have done in this work)
2. Derive a reference ratio between the area under the exponential growth of current or voltage and an area that would be occupied if the signal would have constant steady state value at the reference time.
3. Define accumulator memory variables for area and time
4. Sample a data point with converter and add to the area accumulator product of amplitude of analyzed signal and time between samples. Add time between samples to the time accumulator.
5. If the ratio between the area accumulator and product of actual sample amplitude and time accumulator is more than or equal to the reference ratio proclaim the time accumulator as a scaled time constant of the switched load. Since we define the scaling factor in the beginning of the algorithm time constant can be calculated. If recommended 5 time constant are used as reference time it is possible to use this condition for signalization of steady state to the rest of the program.
6. Otherwise go back to step 4 and continue.

6.2.5 Physical laws with effective values

Limitations: Knowledge that a steady state has been reached

For formative ideas behind the algorithm see Figure 12, tab. 16 and formula (40) in chapter 5.2.2

1. Define two accumulator memory variables for area and one for time
2. Sample a data point of the current and add product of sampled amplitude squared and time between samples to its designated area accumulator
3. Sample a data point of the voltage and add product of of sampled amplitude squared and time between samples to its designated area accumulator
4. Add time between samples to the time accumulator
5. If steady state is reached divide both area accumulators with time accumulator and take square root of both resulting values to acquire effective values of voltage and current. Compute ratio between effective voltage and current to get effective resistance.
6. Otherwise go to step 2 and continue

6.2.6 Energetic

Limitations: Knowledge that steady state has been reached, Data follows resulting circuit equation, Knowledge of steady state parameters

For formative ideas behind the algorithm see formulas (25), (26), (27), (31), (32), (33) in chapters 5.1.2, 5.2.1

1. Define accumulator memory variable for computed energy
2. Derive fundamental circuit equation for signals causing energy accumulation in a circuit component and use it to express the energy then solve it for time constant
3. Sample a data point of the voltage and current at the same time
4. Compute absolute delta value of samples of signal causing energy accumulation with respect to its steady state value
5. Compute actual power from the resulting delta and related signal counterpart (current or voltage)
6. After steady state is reached the time constant is directly calculated by using the derived energy formula for time constant from step 2
7. Otherwise go to step 3 and continue.

6.2.7 Direct point-by-point averaged time constant calculation

Limitations: Data follows exponential transient characteristic, Knowledge of steady state amplitude

For formative ideas behind this algorithm see formulas (36), (37) in chapter 5.2.1

1 Express time constant directly from governing circuit equation

2 Define an accumulator memory variables for time constant and counter

3 Define averaging range of transient amplitude over which an average will be taken.

4 Sample amplitude of the analyzed signal

5 Wait until sampled amplitude enters the defined averaging range then add each computed time constant to the accumulator and increase counter by one.

6 If the next sampled amplitude is outside the averaging range then compute the ratio between time constant accumulator and counter and proclaim it the time constant of the switched load.

7 Otherwise go to step 3 and continue

7 Results

TAB. 17: SUMMARY OF LOAD PARAMETER DETECTION METHODS

Method	Scope of use	Condition	Principle and limitations
Hardware	Inductive - conclusive on→off Capacitive - inconclusive off→on - auxiliary to Integral method Incandescent (off→on) - inconclusive off→on - auxiliary to Integral method Resistive - conclusive off→on→off	Inductive: DEMAG pin changes state from high to low when load is switched off Capacitive/Incandescent: FLT2 pin changes state from low to high when load is switched on Resistive: Neither pin gets triggered in an on/off cycle	For inductive load see chapter 4.1.2. For capacitive and incandescent loads see see FLT2 pin function here 4.1.1 then for more context [40]. Limitation of this approach is that it is hard wired, the quality of detection is hardware dependent. For related algorithm see 6.1.1
Integral ratio	Inductive - conclusive off→on - auxiliary to Hardware method Capacitive - inconclusive on→off - auxiliary to Hardware method Incandescent - inconclusive on→off - auxiliary to Hardware method Resistive - conclusive on/off - auxiliary to Hardware method	Inductive: Ratio between cumulative area under the current curve to the cumulative area occupied by steady state current reaches trigger value and time constant is greater than resistive threshold. Capacitive: Ratio between cumulative area under the inverted voltage curve to the cumulative area under the steady state voltage reaches trigger value and time constant is greater than resistive threshold. Resistive/Incandescent: Ratio between cumulative area under the inverted voltage curve to the cumulative area under the steady state voltage reaches trigger value and time constant is less than or equal to resistive threshold.	For inductive and resistive loads see Figure 11, (22), (23) in chapter 5.1.2. For capacitive, resistive and incandescent loads see analogous derivation (38), (39) in 5.2.2. For limitations and related algorithms see 6.1.1, 6.1.2, 6.2.4

TAB. 18: SUMMARY OF LOAD PARAMETER DETERMINATION METHODS

Method	Scope of use	Principle and limitations
Trivial physical laws	Resistance determination	See formula (15) in chapter 5.1.1 For limitations and related algorithm see 6.2.1
Regression fit parameters	Inductance determination Capacitance determination	See formulas, (18), (19), (34), (35) and tab. 7, tab. 13 in chapter 5.1.2, 5.2.1 For limitations and related algorithm see 6.2.2
Time constant determination at known exponential level	Inductance determination Capacitance determination	See Figure 10 and formulas (20) and (21) in chapter 5.1.2 For limitations and related algorithm see 6.2.3
Integral ratio	Inductance determination	See Figure 11 and formulas (22), (23), (24), (38), (39) in chapters 5.1.2, 5.2.2 For limitation and related algorithm see 6.2.4
Physical laws with effective values	Effective resistance determination	See Figure 12, tab. 16 and formula (40) in chapter 5.2.2 For limitations and related algorithm see 6.2.5
Energetic	Inductance determination Capacitance determination	See formulas (25), (26), (27), (31), (32), (33) in chapters 5.1.2, 5.2.1 For limitations and related algorithm see 6.2.6
Direct point by point averaged time constant calculation	Inductance determination Capacitance determination	See formulas (36), (37) in chapter 5.2.1 For limitations and related algorithm see 6.2.7

Conclusion

Introduction of this work posed a question if it is possible to find a technical solution to automatic detection and switching of typical load types mostly represented by industrial actuators and determination of their parameters of resistance, inductance and capacitance by analyzing the fundamental signals of voltage and current when the load is switched. For that reason I first acquainted myself with various types of commonly used industrial actuators and taken note of characteristic parameters for them and made a theoretical models of such loads supported by simulation.

Next was the feasibility evaluation of available hardware for such task which resulted in discovery of variety of suitable components and designs such as analog to digital converters, analog metering, switches with intelligent features, signal processors and other components for protection and isolation to interface with a digital evaluation electronics. This showed that the proposed idea is definitely feasible.

With knowledge acquired by researching the preliminary requirements I started to design a hardware measurement sample using the STMicroelectronics switch IPS1025H with advanced diagnostic functions and fast demagnetization of inductive loads. The most notable added value of this design was inclusion of demagnetization detecting circuit which can be used in detection procedures and is a suitable complement to the overload diagnostic provided by the switch for inrush currents produced by capacitive loads. In addition I had already available evaluation board STEVAL-FSM01M1 with added feature of analog to digital converter section which I kept in mind as a target environment for my technical solution and possible target for improvements. However the bulk of measurements has been done using the new design and treating an oscilloscope measurement as an equivalent to converter sampling.

Measurement experiments paved a way to deeper conceptual thinking about the technical solution and gave rise to ideas and methods for both detection of the type of switched load as well as determination of its parameters. This was achieved by synthesizing theoretical models from the introduction of work and to apply them to the measured data while making them practical to calculate. These methods where then a blueprint for implementation of their algorithmic counterparts transcribing the methods into a sequence of instruction steps suitable for computation environment.

Results in terms of detection include two detection methods one based on the hardware design and relying on the ability of the switch to detect loads and other on a ratio of integrals which is universal and can be used even for determination of parameters of the switched load and give rise to two detection algorithms. One hybrid of the two methods for detection of type of the electrical loads since the two methods complement each other in many ways and one purely based on the notion of the integral ratio for detection of steady state. Results in terms of determination of switched load parameters are 7 methods giving rise to 7 algorithms implementing them. Each method has unique way of computing the fundamental parameters of inductance, capacitance and resistance and its own set of limitations.

In terms of improvements I would definitely integrate some current measuring section in the next iteration of the hardware design. Another idea improvement would include frequency analysis since analysis done in this work was carried out entirely in the time domain it would be interesting next step to also include frequency domain analysis and see if it improves or even surpasses the currently achieved results.

Bibliography

[1] E. Rice, "Connect automation to the power of predictive maintenance," Control Engineering. Accessed: Jan. 02, 2024. [Online]. Available: https://www.controleng.com/articles/connect-automation-to-the-power-of-predictive-maintenance/

[2] D. Schultz, "How to Implement Predictive Maintenance." Accessed: Jan. 02, 2024. [Online]. Available: https://blog.isa.org/how-to-implement-predictive-maintenance

[3] S. Joshi, "Predictive Maintenance in Cement Manufacturing," Birlasoft. Accessed: Jan. 02, 2024. [Online]. Available: https://www.birlasoft.com/articles/predictive-maintenance-in-cement-manufacturing

[4] D. Jones, "IoT-based predictive maintenance staves off machine failures | TechTarget," IoT Agenda. Accessed: Jan. 02, 2024. [Online]. Available: https://www.techtarget.com/iotagenda/feature/IoT-based-predictive-maintenance-staves-off-machine-failures

[5] E. de Boer et al., "Advanced manufacturing and the promise of Industry 4.0 | McKinsey." Accessed: Jan. 02, 2024. [Online]. Available: https://www.mckinsey.com/capabilities/operations/our-insights/transforming-advanced-manufacturing-through-industry-4-0

[6] C. Coleman et al., "Making maintenance smarter," Deloitte Insights. Accessed: Jan. 02, 2024. [Online]. Available: https://www2.deloitte.com/content/www/us/en/insights/focus/industry-4-0/using-predictive-technologies-for-asset-maintenance.html

[7] S. Cavalieri and M. G. Salafia, "A Model for Predictive Maintenance Based on Asset Administration Shell," *Sensors*, vol. 20, no. 21, p. 6028, Oct. 2020, doi: 10.3390/s20216028.

[8] Y. Ran, X. Zhou, P. Lin, Y. Wen, and R. Deng, "A Survey of Predictive Maintenance: Systems, Purposes and Approaches." arXiv, Dec. 12, 2019. Accessed: Oct. 23, 2023. [Online]. Available: http://arxiv.org/abs/1912.07383

[9] J. Lee, J. Ni, J. Singh, B. Jiang, M. Azamfar, and J. Feng, "Intelligent Maintenance Systems and Predictive Manufacturing," *J. Manuf. Sci. Eng.*, vol. 142, no. 110805, Aug. 2020, doi: 10.1115/1.4047856.

[10] A. Cachada *et al.*, "Maintenance 4.0: Intelligent and Predictive Maintenance System Architecture," in *2018 IEEE 23rd International Conference on Emerging Technologies and Factory Automation (ETFA)*, Sep. 2018, pp. 139–146. doi: 10.1109/ETFA.2018.8502489.

[11] F. Alves *et al.*, "Deployment of a Smart and Predictive Maintenance System in an Industrial Case Study," in *2020 IEEE 29th International Symposium on Industrial Electronics (ISIE)*, Jun. 2020, pp. 493–498. doi: 10.1109/ISIE45063.2020.9152441.

[12] M. Achouch *et al.*, "On Predictive Maintenance in Industry 4.0: Overview, Models, and Challenges," *Appl. Sci.*, vol. 12, no. 16, Art. no. 16, Jan. 2022, doi: 10.3390/app12168081.

[13] K. S. H. Ong, W. Wang, N. Q. Hieu, D. Niyato, and T. Friedrichs, "Predictive Maintenance Model for IIoT-Based Manufacturing: A Transferable Deep Reinforcement Learning Approach," *IEEE Internet Things J.*, vol. 9, no. 17, pp. 15725–15741, Sep. 2022, doi: 10.1109/JIOT.2022.3151862.

[14] M. Cakir, M. A. Guvenc, and S. Mistikoglu, "The experimental application of popular machine learning algorithms on predictive maintenance and the design of IIoT based condition monitoring system," *Comput. Ind. Eng.*, vol. 151, p. 106948, Jan. 2021, doi: 10.1016/j.cie.2020.106948.

[15]S. Ayvaz and K. Alpay, "Predictive maintenance system for production lines in manufacturing: A machine learning approach using IoT data in real-time," *Expert Syst. Appl.*, vol. 173, p. 114598, Jul. 2021, doi: 10.1016/j.eswa.2021.114598.
[16]P. Jieyang *et al.*, "A systematic review of data-driven approaches to fault diagnosis and early warning," *J. Intell. Manuf.*, Sep. 2022, doi: 10.1007/s10845-022-02020-0.
[17]H. Fu and Y. Liu, "A deep learning-based approach for electrical equipment remaining useful life prediction," *Auton. Intell. Syst.*, vol. 2, no. 1, p. 16, Jul. 2022, doi: 10.1007/s43684-022-00034-2.
[18]J.-R. Ruiz-Sarmiento, J. Monroy, F.-A. Moreno, C. Galindo, J.-M. Bonelo, and J. Gonzalez-Jimenez, "A predictive model for the maintenance of industrial machinery in the context of industry 4.0," *Eng. Appl. Artif. Intell.*, vol. 87, p. 103289, Jan. 2020, doi: 10.1016/j.engappai.2019.103289.
[19]K. T. P. Nguyen and K. Medjaher, "A new dynamic predictive maintenance framework using deep learning for failure prognostics," *Reliab. Eng. Syst. Saf.*, vol. 188, pp. 251–262, Aug. 2019, doi: 10.1016/j.ress.2019.03.018.
[20]J. Zenisek, F. Holzinger, and M. Affenzeller, "Machine learning based concept drift detection for predictive maintenance," *Comput. Ind. Eng.*, vol. 137, p. 106031, Nov. 2019, doi: 10.1016/j.cie.2019.106031.
[21]V. Justus and G. R. Kanagachidambaresan, "Machine learning based fault-oriented predictive maintenance in industry 4.0," *Int. J. Syst. Assur. Eng. Manag.*, Sep. 2022, doi: 10.1007/s13198-022-01777-0.
[22]J. Sharma, M. L. Mittal, and G. Soni, "Condition-based maintenance using machine learning and role of interpretability: a review," *Int. J. Syst. Assur. Eng. Manag.*, Dec. 2022, doi: 10.1007/s13198-022-01843-7.
[23]N. M. Thoppil, V. Vasu, and C. S. P. Rao, "Deep Learning Algorithms for Machinery Health Prognostics Using Time-Series Data: A Review," *J. Vib. Eng. Technol.*, vol. 9, no. 6, pp. 1123–1145, Sep. 2021, doi: 10.1007/s42417-021-00286-x.
[24]"Predictive Maintenance (PdM) with Smart Motor Sensor - ADI OtoSense." Accessed: Jan. 02, 2024. [Online]. Available: https://otosense.analog.com/
[25]"GE Digital's SmartSignal Predictive Maintenance Software Solution Features 'Time-to-Action' Forecast Analytics | GE News." Accessed: Jan. 02, 2024. [Online]. Available: https://www.ge.com/news/press-releases/ge-digitals-smartsignal-predictive-maintenance-software-features-time-to-value
[26]"EVM430-I2040S Evaluation board | TI.com." Accessed: Jan. 02, 2024. [Online]. Available: https://www.ti.com/tool/EVM430-I2040S
[27]"TIPD121 reference design | TI.com." Accessed: Jan. 02, 2024. [Online]. Available: https://www.ti.com/tool/TIPD121
[28]"CN0549 Circuit Note | Analog Devices." Accessed: Jan. 02, 2024. [Online]. Available: https://www.analog.com/en/design-center/reference-designs/circuits-from-the-lab/cn0549.html
[29]"TIDA-01552 reference design | TI.com." Accessed: Jan. 02, 2024. [Online]. Available: https://www.ti.com/tool/TIDA-01552
[30]I. T. AG, "REF-ISOH812G-I813T - Infineon Technologies." Accessed: Jan. 02, 2024. [Online]. Available: https://www.infineon.com/cms/en/product/isolation/isolated-industrial-interface/ref-isoh812g-i813t/
[31]"Evaluation Kit – ABS and ESP." Accessed: Jan. 02, 2024. [Online]. Available: https://www.nxp.com/products/power-management/smart-switches-and-drivers/low-side-switches/evaluation-kit-valves-controller-soc:KITVALVECNTLEVM
[32]"STEVAL-BFA001V2B - Multi-sensor predictive maintenance kit with IO-Link stack v.1.1 - STMicroelectronics." Accessed: Jan. 08, 2024. [Online]. Available: https://www.st.com/en/evaluation-tools/steval-bfa001v2b.html

[33]"MAXREFDES278 | reference design | Analog Devices." Accessed: Jan. 02, 2024. [Online]. Available: https://www.analog.com/en/design-center/reference-designs/maxrefdes278.html
[34]"EVAL-ADMX2001 Evaluation Board | Analog Devices." Accessed: Jan. 02, 2024. [Online]. Available: https://www.analog.com/en/design-center/evaluation-hardware-and-software/evaluation-boards-kits/eval-admx2001.html
[35]You Chung Chung, N. N. Amarnath, and C. M. Furse, "Capacitance and Inductance Sensor Circuits for Detecting the Lengths of Open- and Short-Circuited Wires," *IEEE Trans. Instrum. Meas.*, vol. 58, no. 8, pp. 2495–2502, Aug. 2009, doi: 10.1109/TIM.2009.2014617.
[36]P. Zhang, *Industrial Control Technology*. William Andrew Publishing, 2008. [Online]. Available: https://doi.org/10.1016/B978-081551571-5.50002-5.
[37]"STEVAL-FSM01M1 - Advanced dual channel digital I/O module for safe automation - STMicroelectronics." Accessed: Jan. 03, 2024. [Online]. Available: https://www.st.com/en/evaluation-tools/steval-fsm01m1.html
[38]"NUCLEO-F401RE - STM32 Nucleo-64 development board with STM32F401RE MCU, supports Arduino and ST morpho connectivity - STMicroelectronics." Accessed: Jan. 03, 2024. [Online]. Available: https://www.st.com/en/evaluation-tools/nucleo-f401re.html
[39]"NUCLEO-G431RB - STM32 Nucleo-64 development board with STM32G431RB MCU, supports Arduino and ST morpho connectivity - STMicroelectronics." Accessed: Jan. 03, 2024. [Online]. Available: https://www.st.com/en/evaluation-tools/nucleo-g431rb.html
[40]"IPS1025H - High efficiency, high-side switch with extended diagnostic and smart driving for capacitive loads - STMicroelectronics." Accessed: Jan. 03, 2024. [Online]. Available: https://www.st.com/en/power-management/ips1025h.html
[41]"SMM4F33A - 400 W, 33 V TVS in STmite Flat - STMicroelectronics." Accessed: Jan. 03, 2024. [Online]. Available: https://www.st.com/en/protections-and-emi-filters/smm4f33a.html
[42]"ACPL-M61L-000E." Accessed: Jan. 03, 2024. [Online]. Available: https://www.broadcom.com/products/optocouplers/industrial-plastic/digital-optocouplers/10mbd/acpl-m61l-000e
[43]V. Eliáš, "Consultation with senior engineer at STMicroelectronics laboratory," 2023.
[44]"STISO620 - Dual channel digital isolator - STMicroelectronics." Accessed: Jan. 03, 2024. [Online]. Available: https://www.st.com/en/interfaces-and-transceivers/stiso620.html
[45]"SM15T36CA - 1500 W, 30.8 V TVS in SMC - STMicroelectronics." Accessed: Jan. 03, 2024. [Online]. Available: https://www.st.com/en/protections-and-emi-filters/sm15t36ca.html
[46]"STPS1L60 - 60 V, 1 A Low Drop Power Schottky Rectifier - STMicroelectronics." Accessed: Jan. 03, 2024. [Online]. Available: https://www.st.com/en/diodes-and-rectifiers/stps1l60.html
[47]"LM2931 - Very low drop voltage regulators with inhibit function - STMicroelectronics." Accessed: Jan. 03, 2024. [Online]. Available: https://www.st.com/en/power-management/lm2931.html
[48]"zunzuncode / pyeq3 / Models__2D / Exponential.py — Bitbucket." Accessed: Jan. 03, 2024. [Online]. Available: https://bitbucket.org/zunzuncode/pyeq3/src/master/Models__2D/Exponential.py
[49]F. svg: S. work: MikeRun, *Deutsch: Zeitverlauf bei der Induktion im Gleichstromkreis*. 2012. Accessed: Jan. 03, 2024. [Online]. Available: https://commons.wikimedia.org/wiki/File:Inductance-current-and-voltage-diagram.svg

Appendix A: Simulations

Legend: Green➔v_1=v_R, Blue➔i

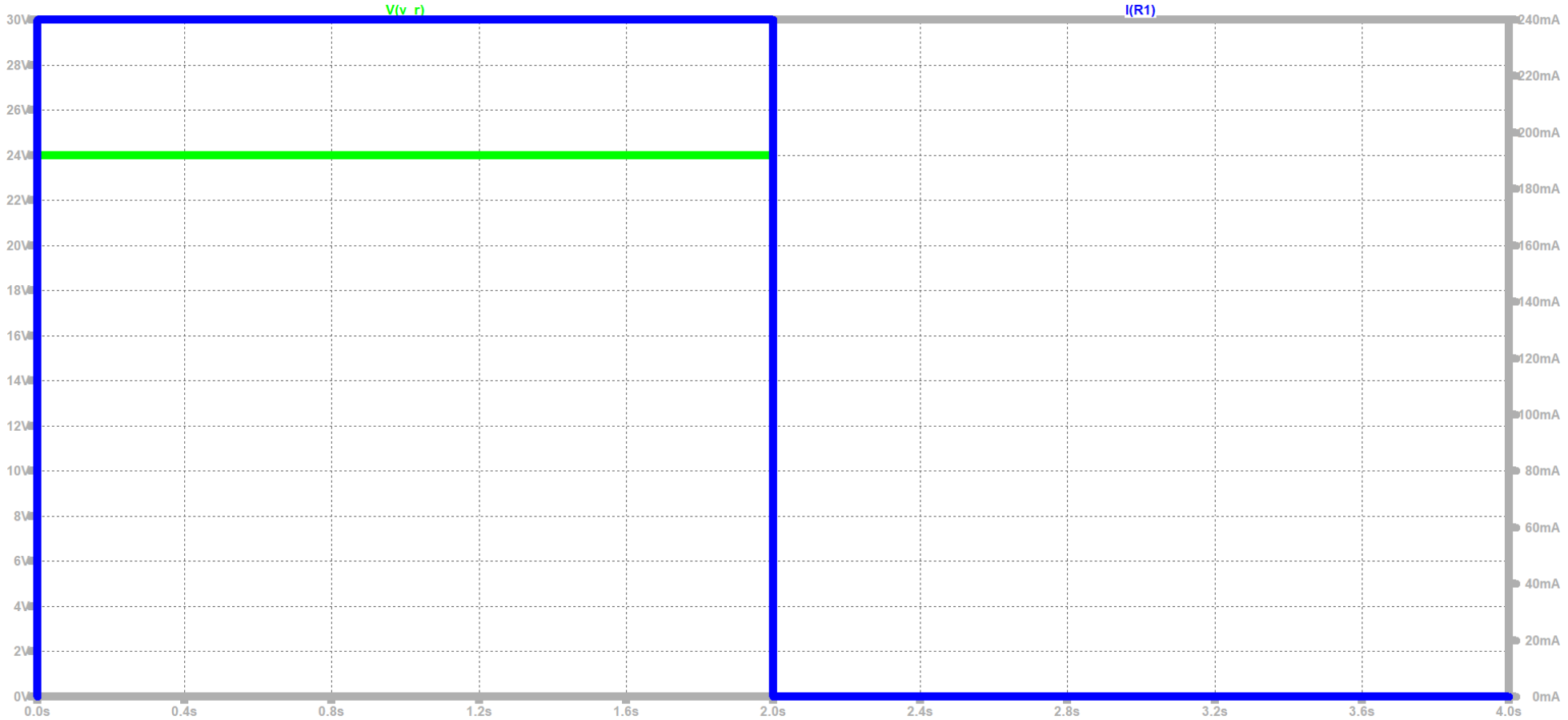

FIGURE A.1: STEP TRANSIENT RESPONSE SIMULATION OF RESISTIVE LOAD

Legend: Green➔v_1, Blue➔v_L, Red➔i

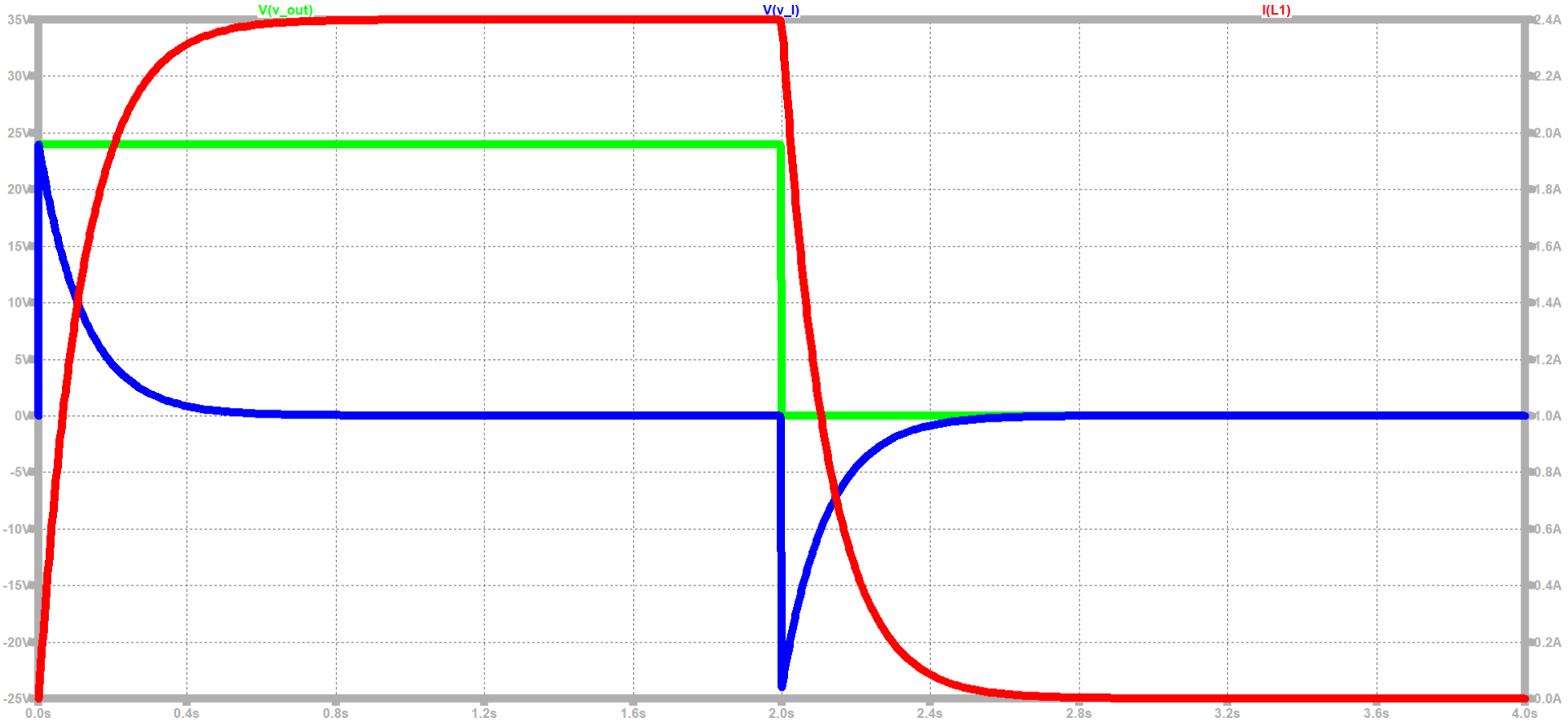

FIGURE A.2: STEP TRANSIENT RESPONSE SIMULATION OF INDUCTIVE LOAD

Legend: Green→v_1, Blue→v_{RC}, Red→i

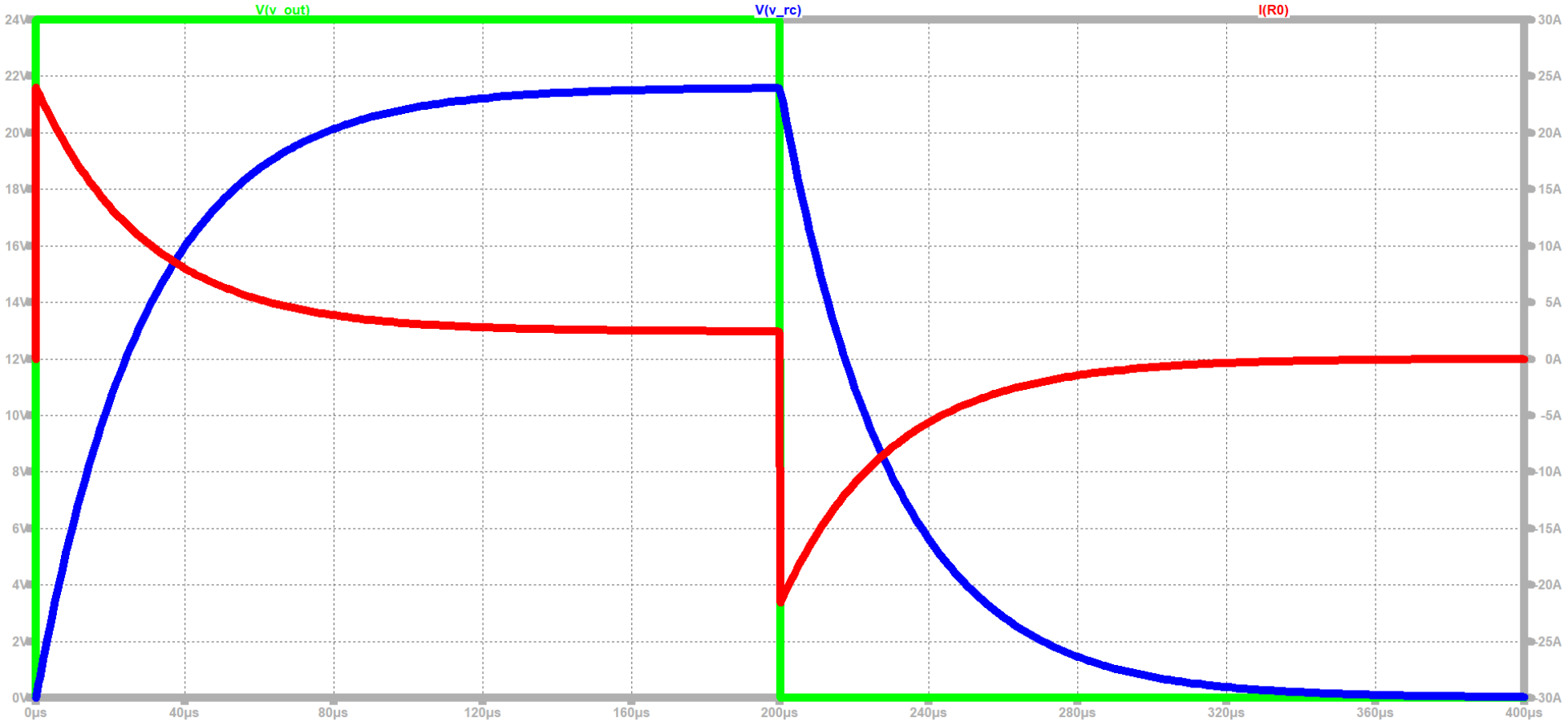

FIGURE A.3: STEP TRANSIENT RESPONSE SIMULATION OF CAPACITIVE LOAD

Appendix B: Additional schematics and hardware design layers

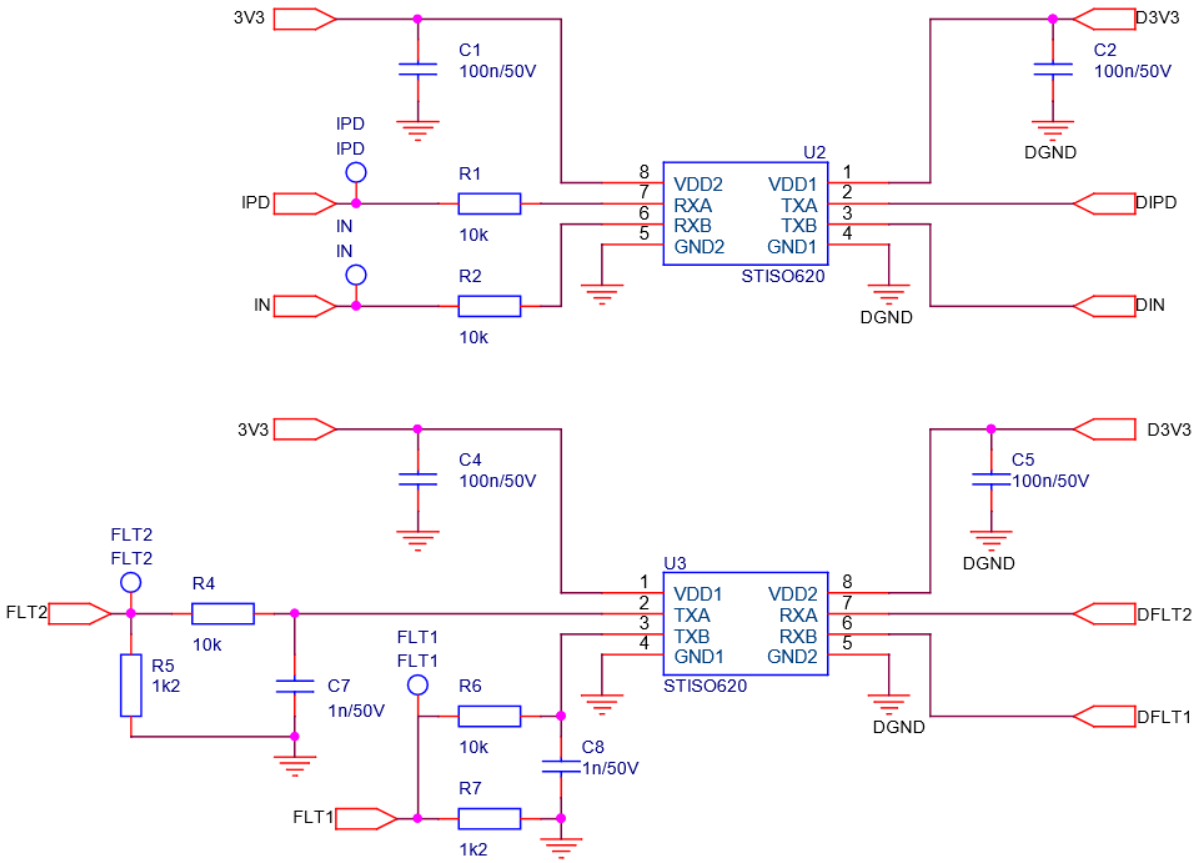

FIGURE B.1: INTERFACE BETWEEN POWER AND DIGITAL PARTS OF THE DESIGN

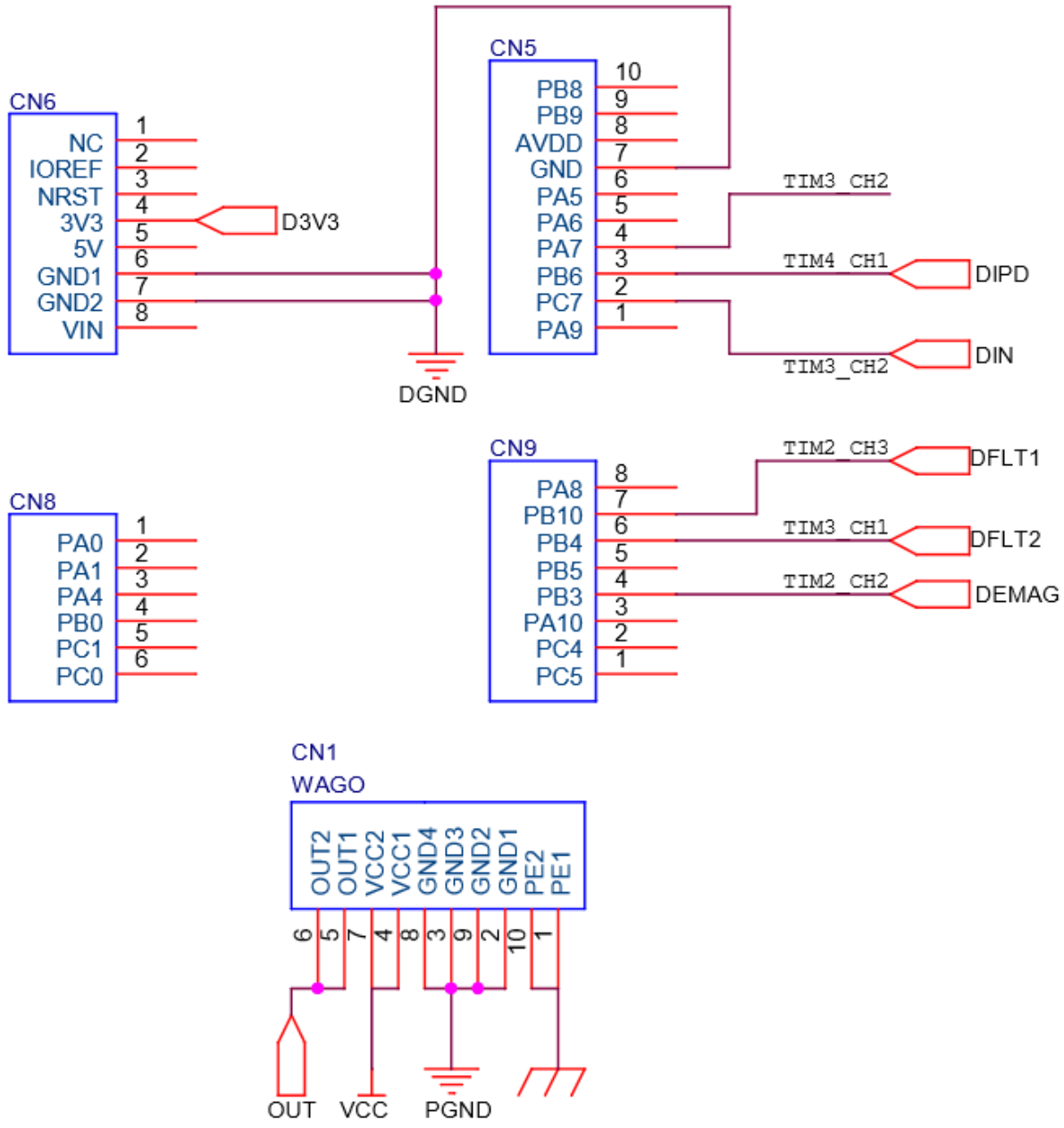

FIGURE B.2: SCHEMATIC FOR PHYSICAL CONNECTORS

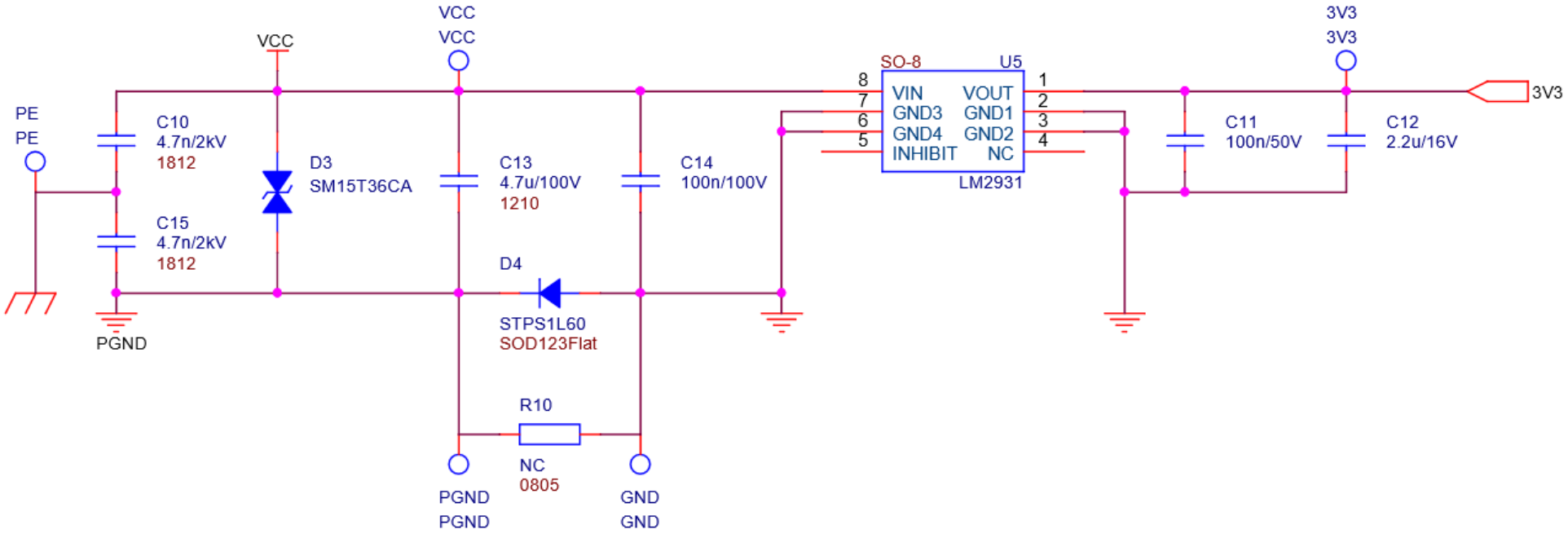

FIGURE B.3: SUPPLY INTERFACE WITH PROTECTIONS

tab. B.1: Components used in hardware sample

Reference	Value	Rating	Manufacturer reference
C1,2,4,5,9,11	100nF	50V	MURATA GCJ188R71H104KA12D
C3,14	100nF	100V	MURATA GRM188R72A104KA35D
C6	22nF	100V	MURATA GRM188R72A223KAC4D
C7,8	1nF	50V	YAGEO CC0603KRX7R9BB102
C10,15	4.7nF	2kV	YAGEO CC1812KKX7RDBB472
C12	2.2µF	16V	-
C13	4.7µF	100V	TDK CNC6P1X7R2A475K250AE
CN1	-	Multiple	WAGO 235-404 and other color permutations
CN5	10pin	6.3A/ 655V	SAMTEC SSQ-110-04-G-S
CN6,9	8pin	6.3A/ 655V	SAMTEC SSQ-108-04-G-S
CN8	6pin	6.3A/ 655V	SAMTEC SSQ-106-04-G-S
D1	Green	20mA	WURTH ELEKTRONIK 150060VS75020
D2	-	400W/ 30kV (PP)	STMICROELECTRONICS SMM4F33A-TR
D3	-	1500W (PP)	STMICROELECTRONICS SM15T36CA
D4	-	60V (RRM)	STMICROELECTRONICS STPS1L60ZF
R1,2,4,6,8	10kΩ	0.1W	YAGEO RC0603JR-0710KL
R3	12kΩ	0.1W	YAGEO RC0603FR-0712KL
R5,7	1.2kΩ	0.1W	-
OUT, DMG, IN, IPD, FLT1, FLT2	Grey	-	KEYSTONE 5118
GND	Black	-	KEYSTONE 5001
VCC, 3V3	Red	-	KEYSTONE 5000
PGND	Blue	-	KEYSTONE 5117
U1	-	65V	STMICROELECTRONICS IPS1025HTR
U2,3	-	5mA/5.5V	STMICROELECTRONICS STISO620TR
U4	-	3.75kV	BROADCOM ACPL-M61L-000E
U5	-	40V	STMICROELECTRONICS LM2931AD33R

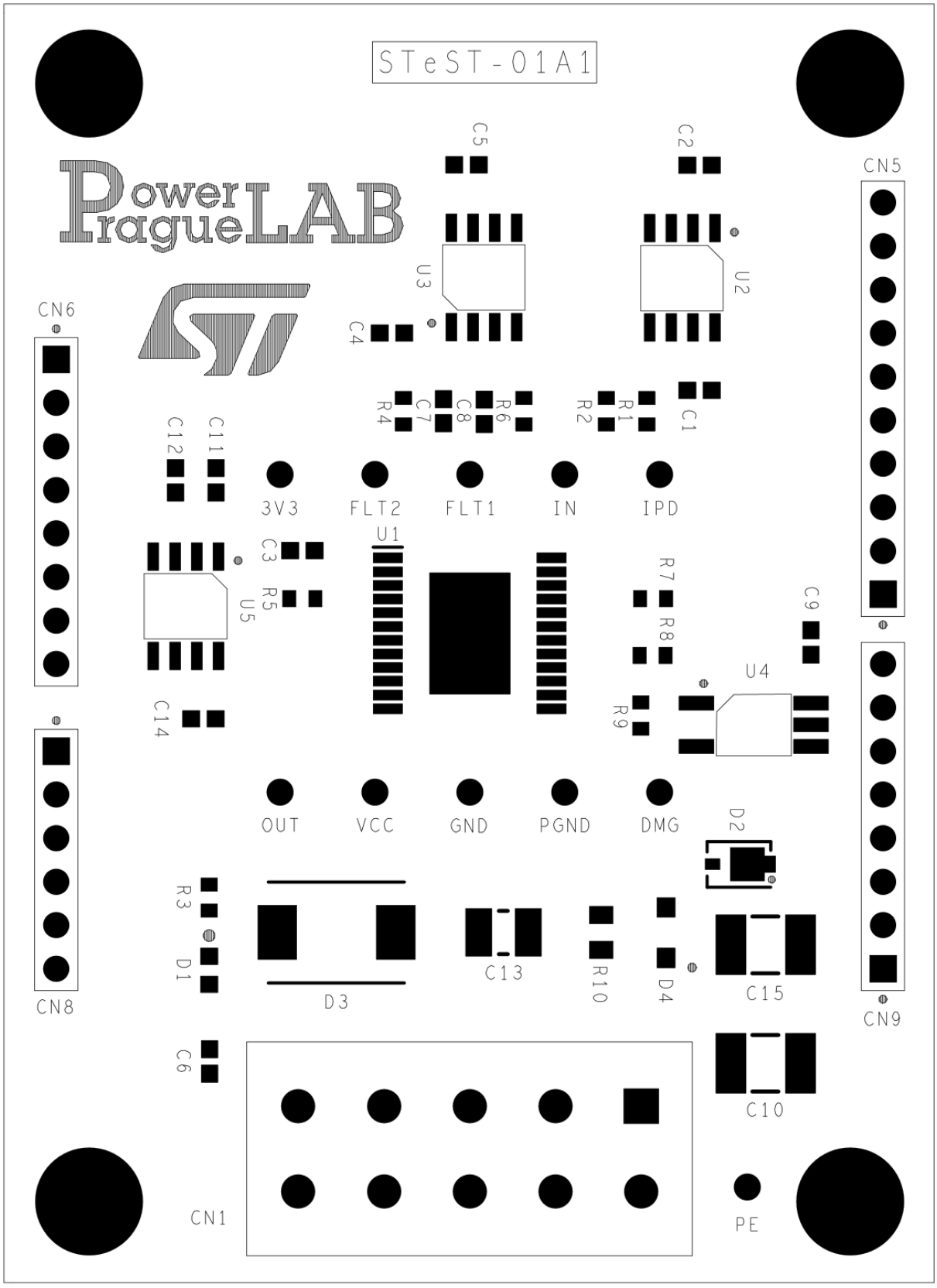

FIGURE B.4: TOP LAYER FOOTPRINT OVERVIEW WITH SILKSCREEN AND MOUNTING HOLES

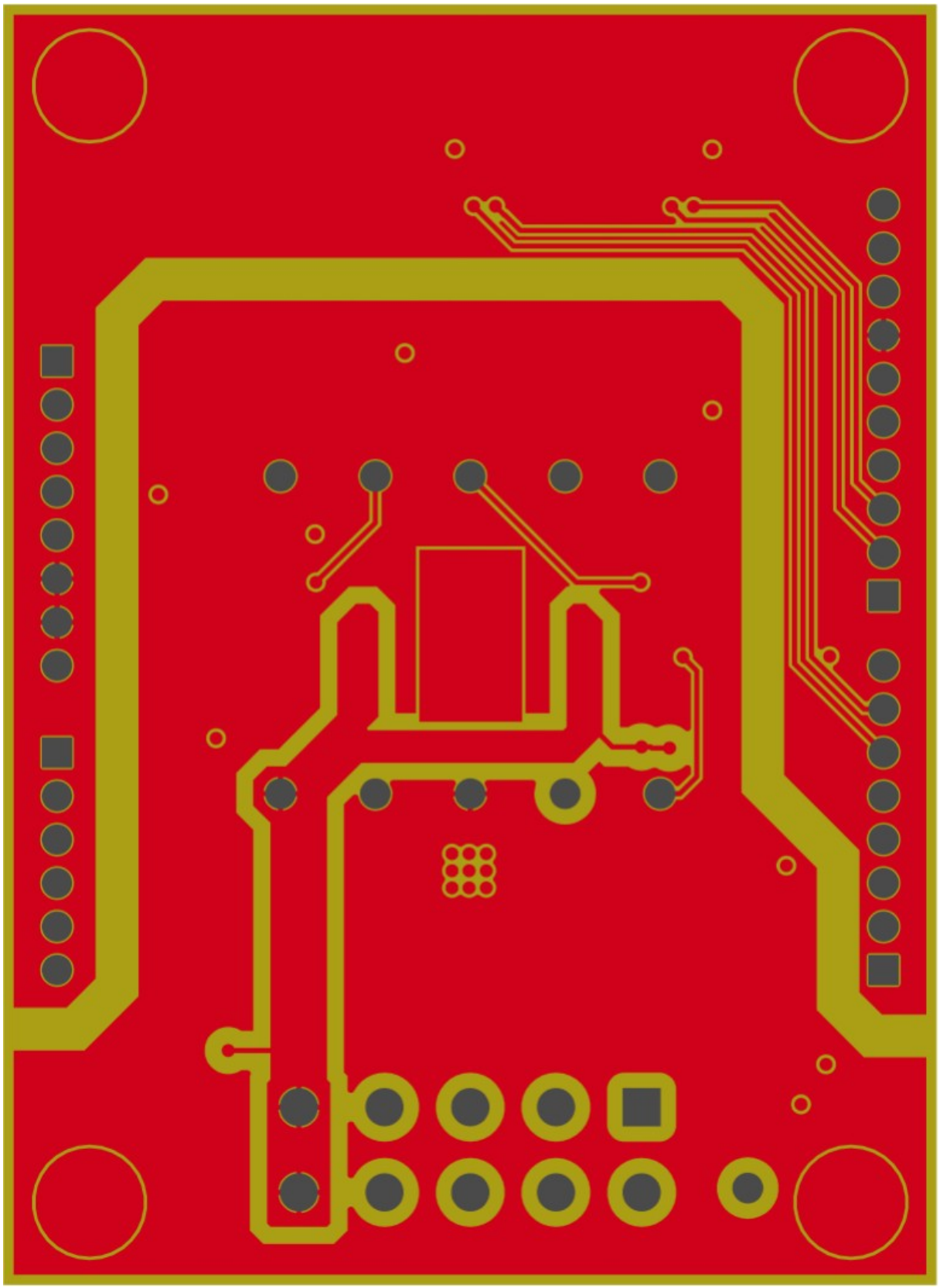

FIGURE B.5: BOTTOM LAYER LAYOUT AND SOLDERMASK

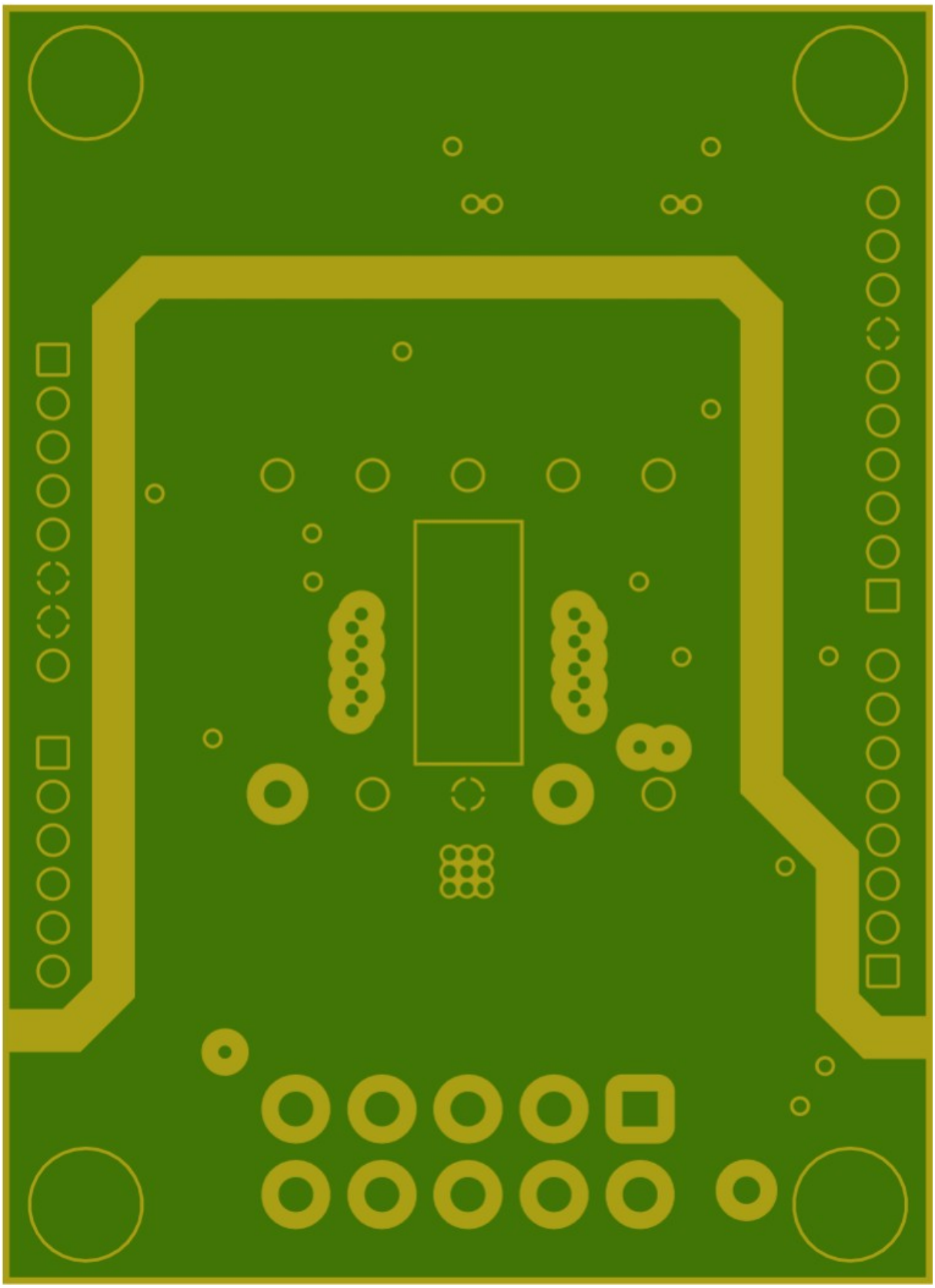

FIGURE B.6: FIRST INNER LAYER LAYOUT

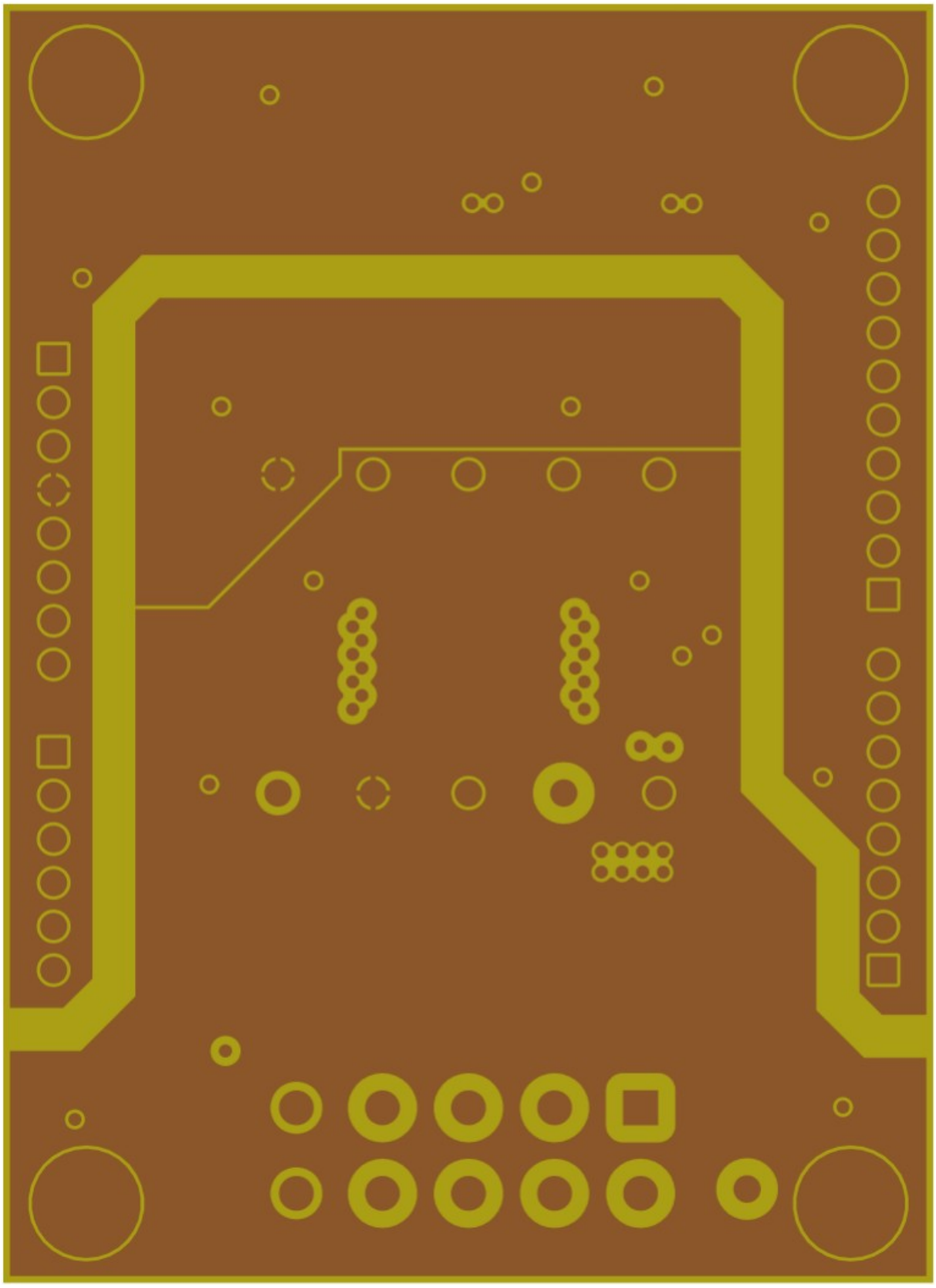

FIGURE B.7: SECOND INNER LAYER LAYOUT

Appendix C: Oscillograms

Legend: Channel 1→V_{CC}, Channel 2→v_1, Channel 4→i

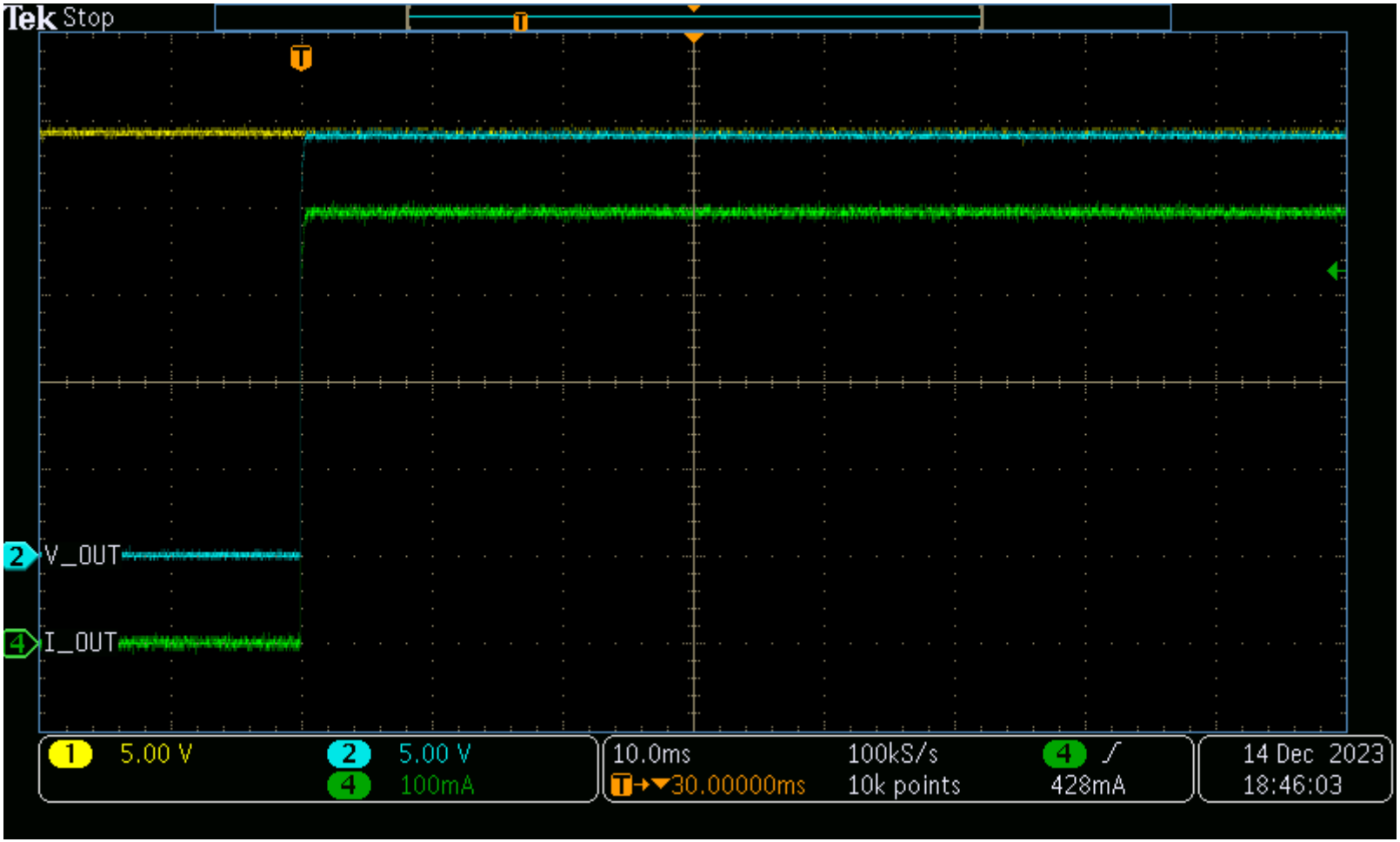

FIGURE C.1: SWITCHING 47Ω RESITOR ON

Legend: Channel 1→V_{CC}, Channel 2→v_1, Channel 4→i

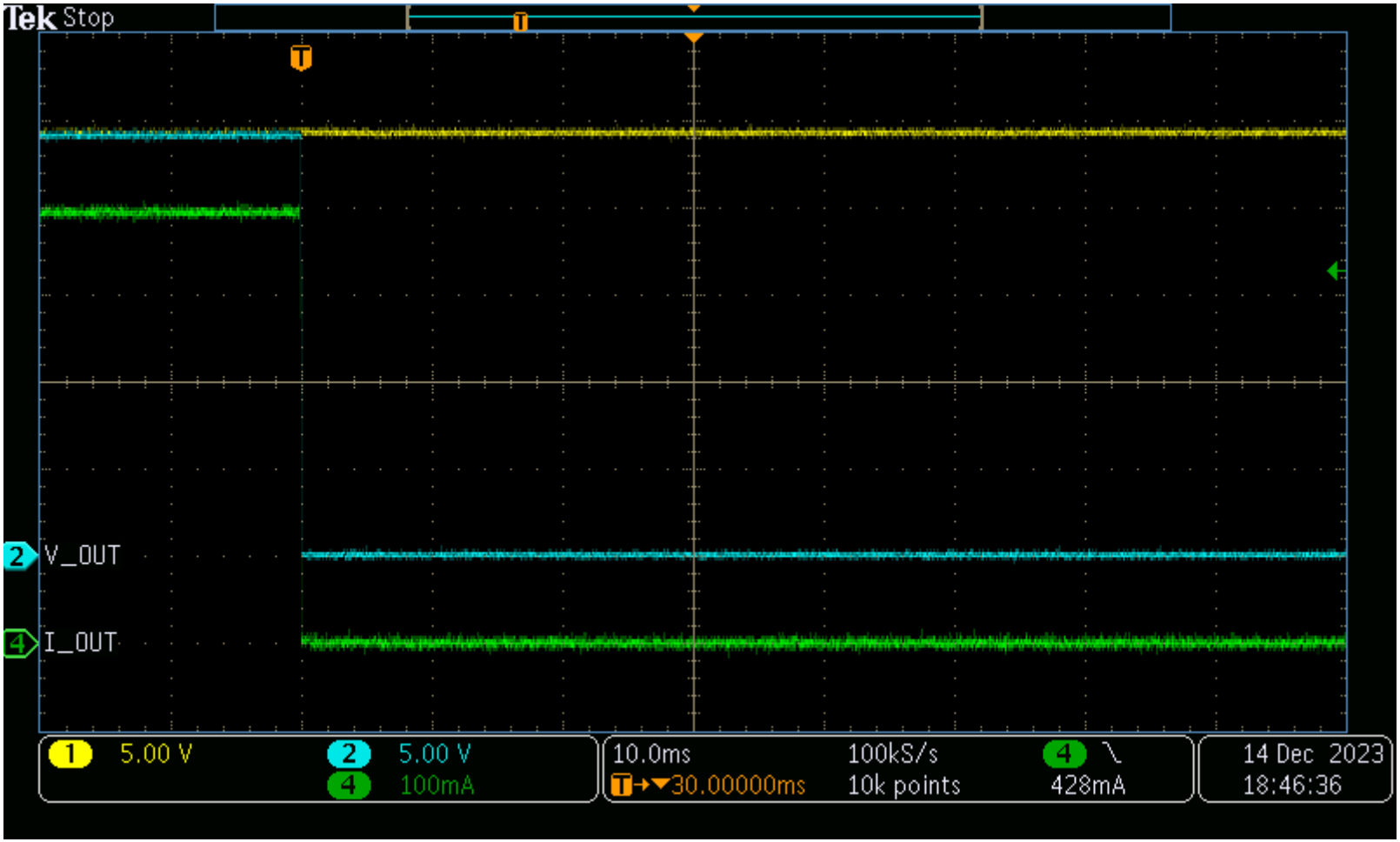

FIGURE C.2: SWITCHING 47Ω RESISTOR OFF

Legend: Channel 1→V_{CC}, Channel 2→v_1, Channel 4→*i, Channel M*→E_{INFLUX}, Channel R2→P_{INFLUX}, Channel R3→I_1

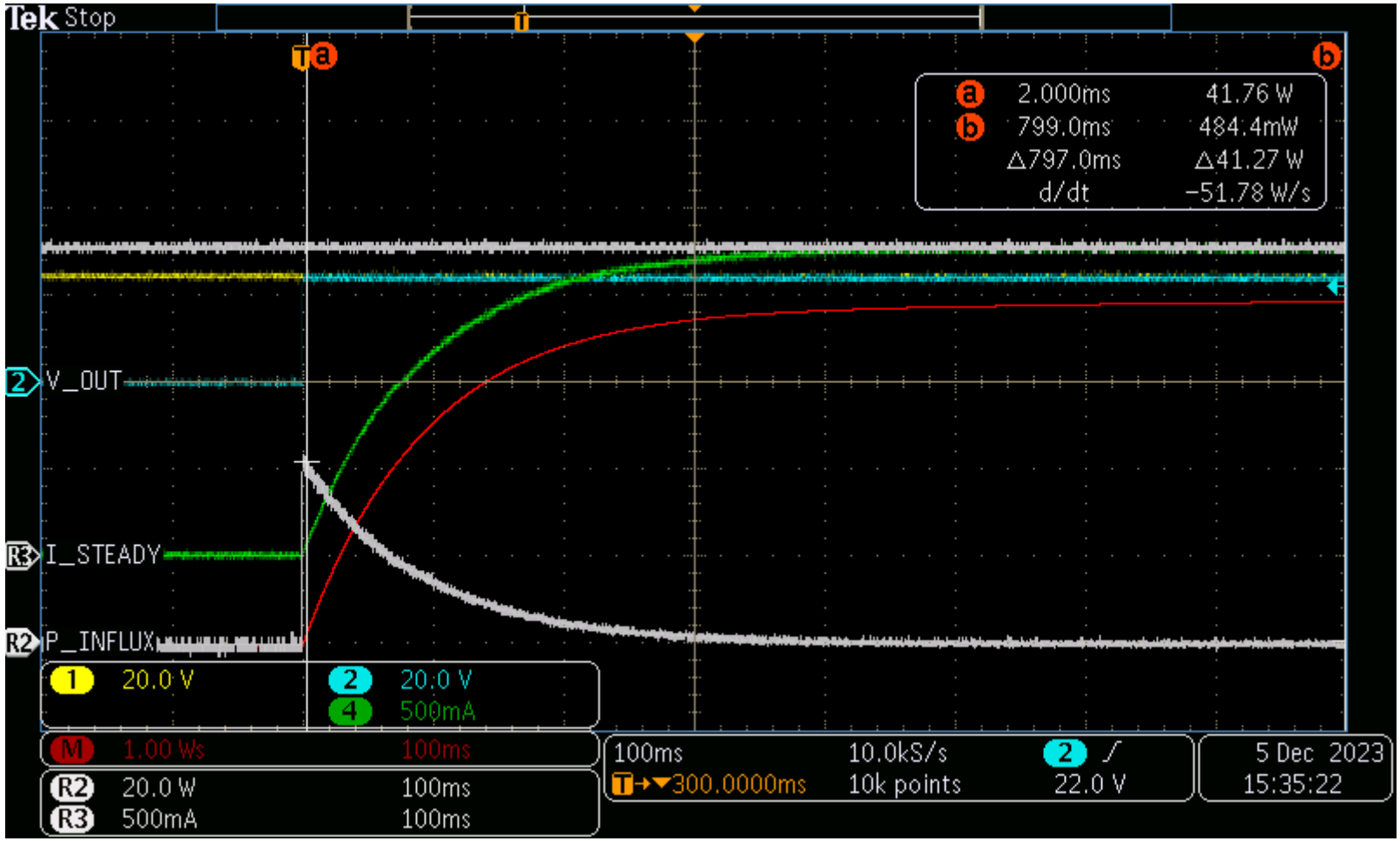

FIGURE C.3: SWITCHING ON A 1.2H(14Ω) INDUCTOR

Legend: Channel 1→V_{CC}, Channel 2→v_1, Channel 4→i, *Channel M*→$E_{DEMAG,}$ Channel R1→E_{SWITCH}, Channel R3→P_{SWITCH}, Channel R4→P_{DEMAG} (saw tooth shaped pulse with lesser maximum)

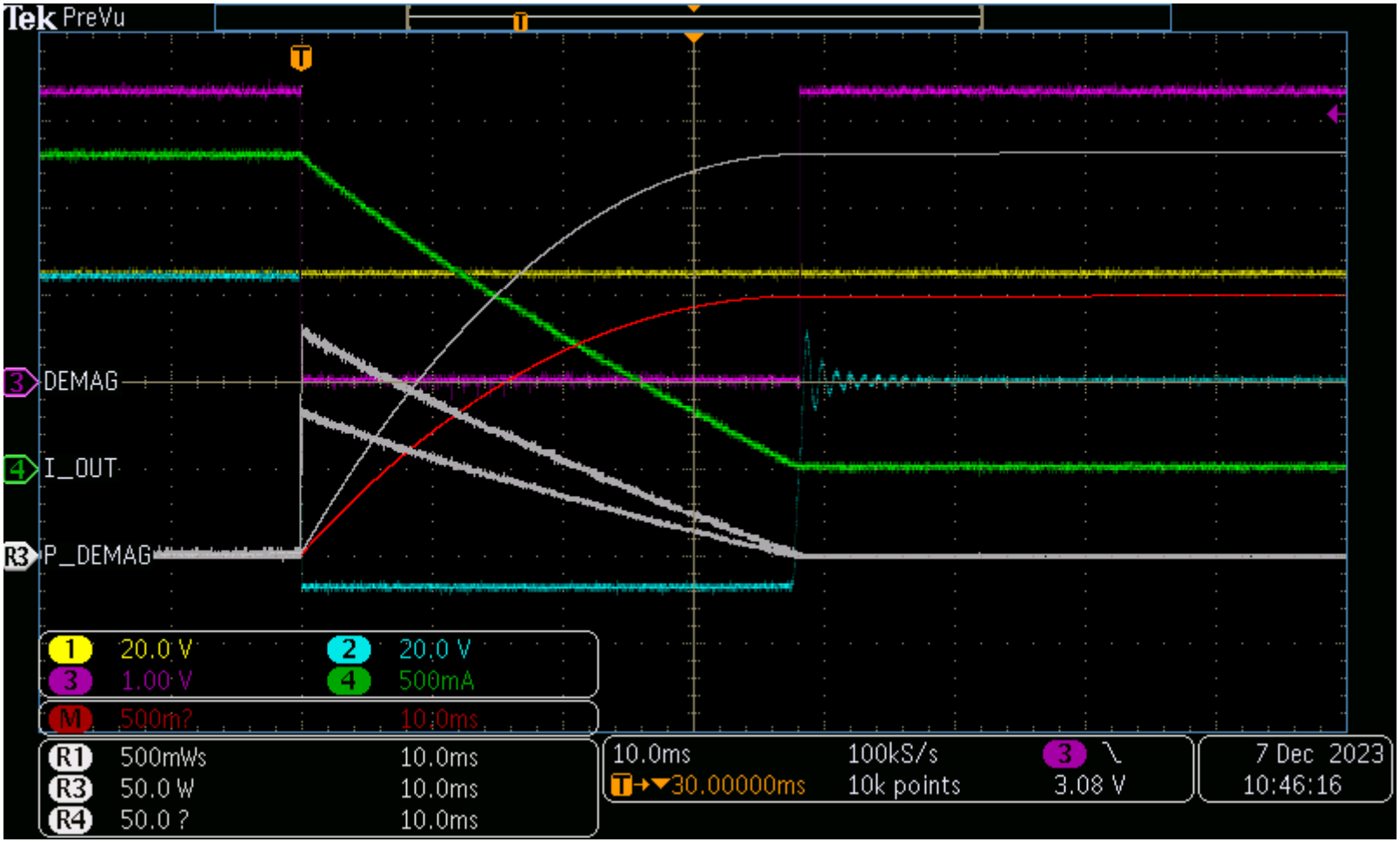

FIGURE C.4: SWITCHING OFF A 1.2H(14Ω) INDUCTOR

Legend: Channel 1→V_{CC}, Channel 2→v_1, Channel 4→i, *Channel M*→E_{INFLUX}, Channel R4→P_{INFLUX}

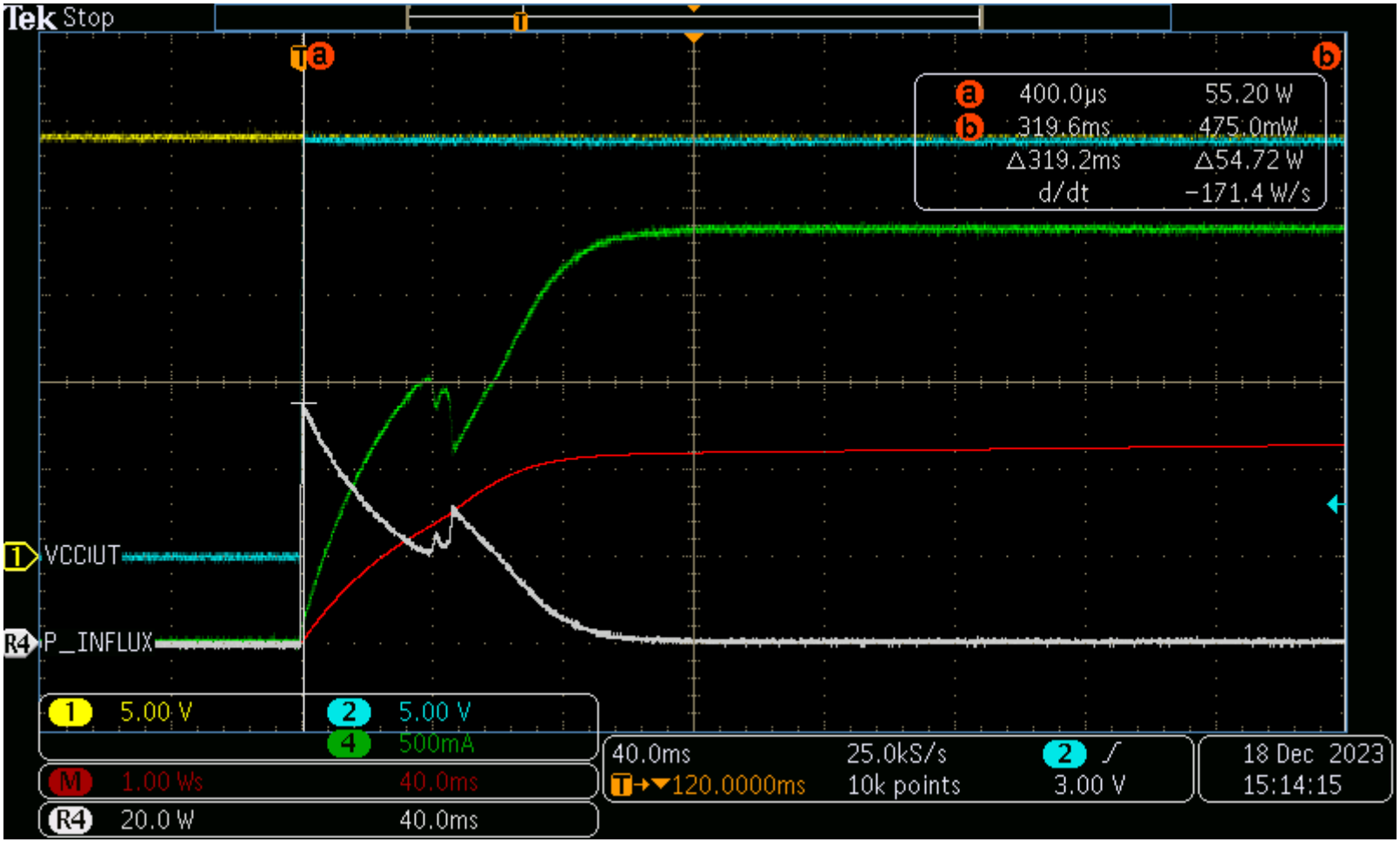

FIGURE C.5: SWITCHING ELECTROMAGNETIC MOTOR BRAKE ON

Legend: Channel 1→V_{CC}, Channel 2→v_1, Channel 4→i, *Channel M*→$E_{DEMAG,}$ Channel R4→P_{DEMAG}

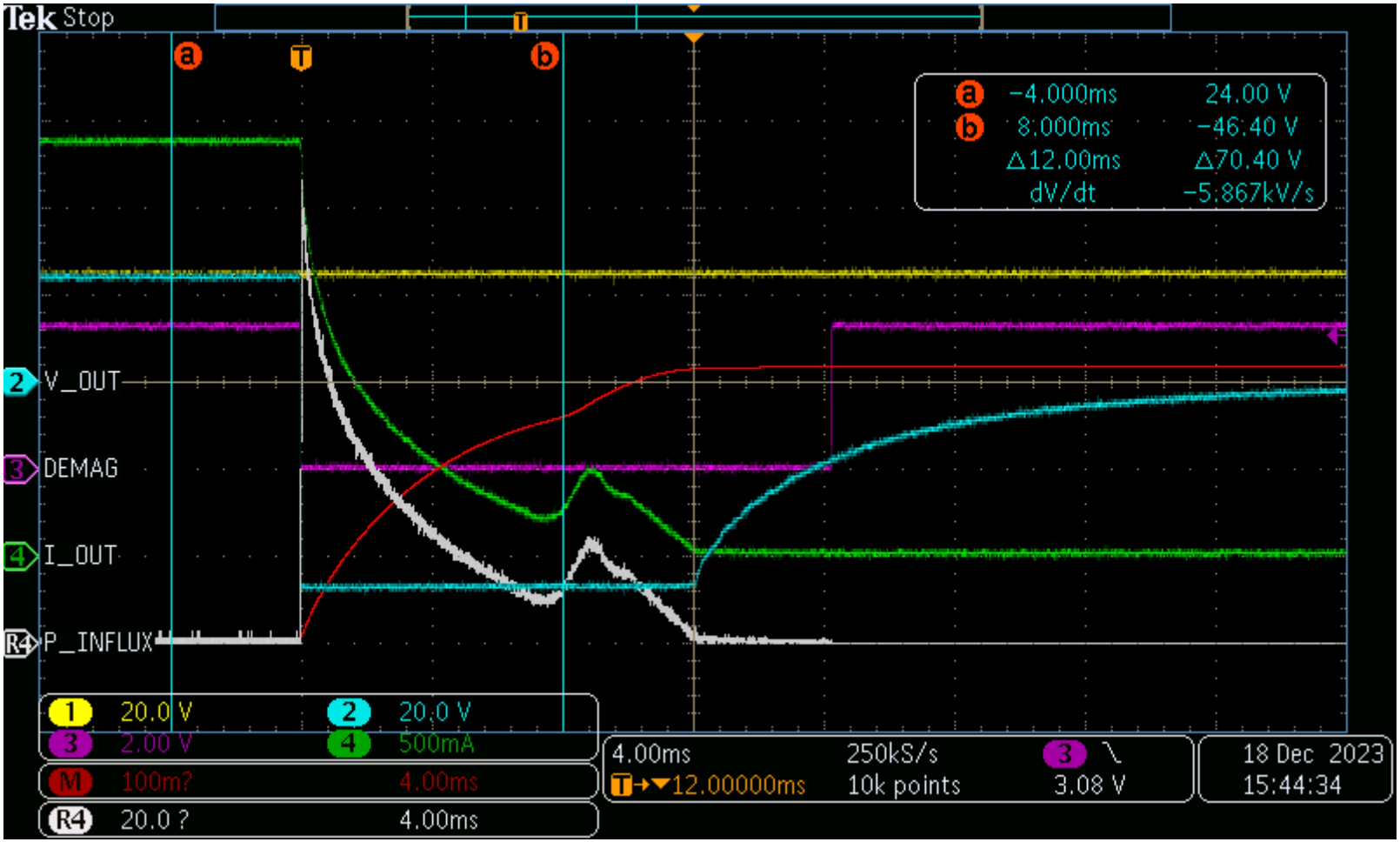

FIGURE C.6: SWITCHING ELECTROMAGNETIC MOTOR BRAKE OFF

Legend: Channel 1→V_{CC}, Channel 2→v_1, Channel 4→*i*, *Channel M*→$E_{INRUSH,}$ Channel R3→P_{INRUSH}, Channel R4→I_1

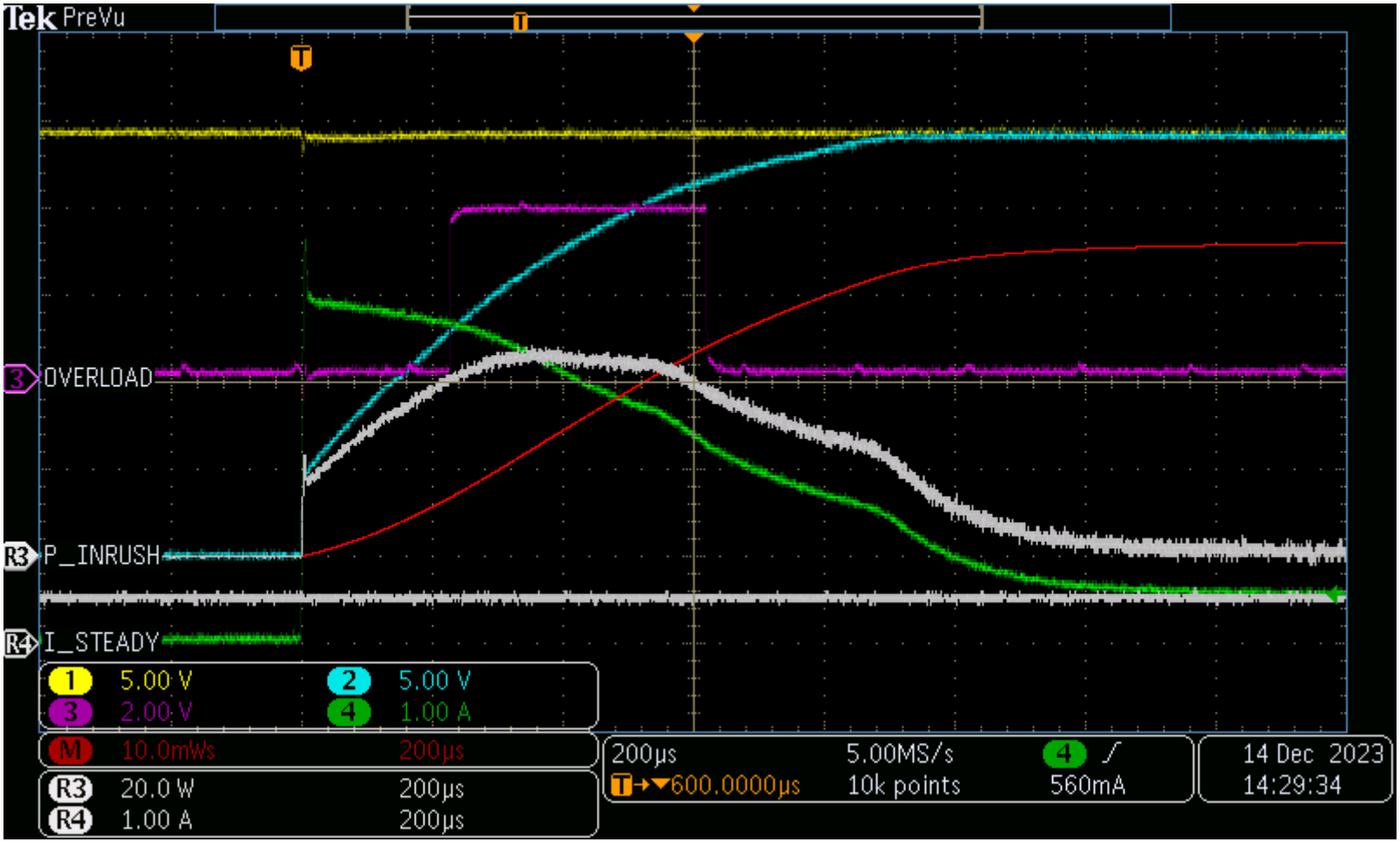

FIGURE C.7: SWITCHING 100MF CAPACITIVE LOAD ON

Legend: Channel 1→V_{CC}, Channel 2→v_1, Channel 4→i

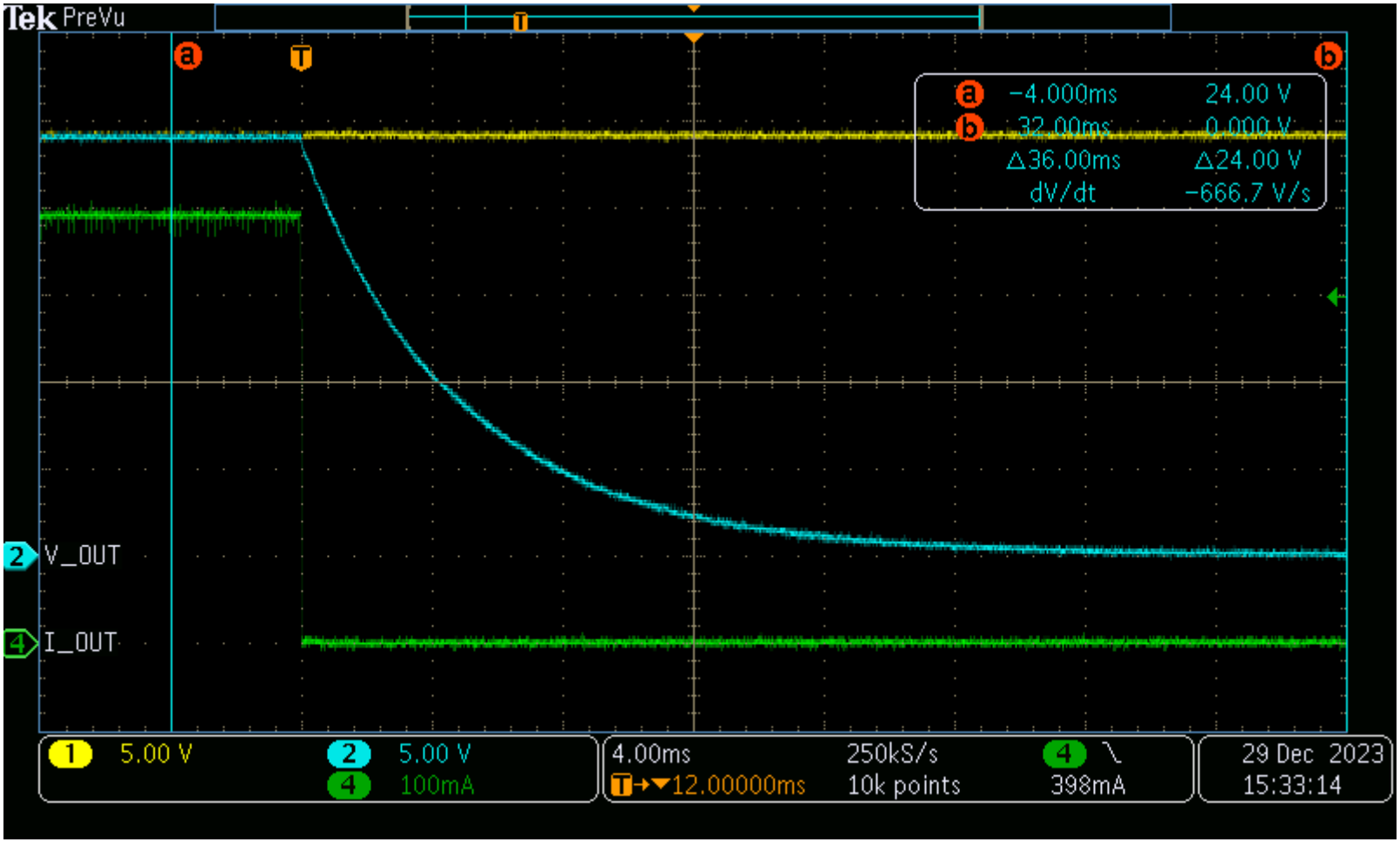

FIGURE C.8: SWITCHING 100MF CAPACITIVE LOAD OFF

Legend: Channel 1→V_{CC}, Channel 2→v_1, Channel 4→*i*, *Channel M*→E_{INRUSH}, Channel R3→P_{INRUSH}

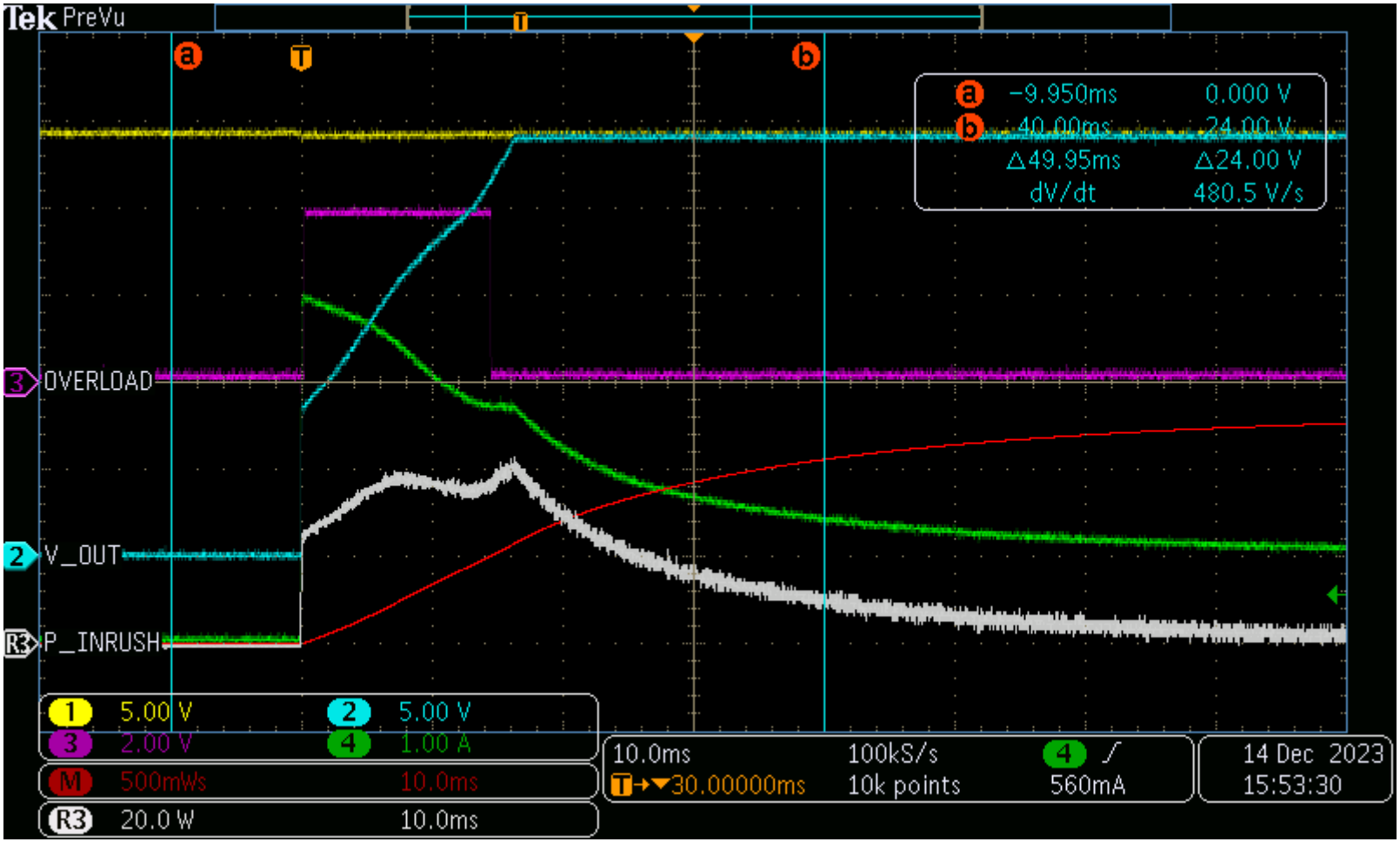

FIGURE C.9: SWITCHING 1A INCANDESCENT LIGHT BULB ON

Legend: Channel 1→V_{CC}, Channel 2→v_1, Channel 4→i, Channel R2→v_1, Channel R3→i, Channels R2, R3 belong to capacitive load

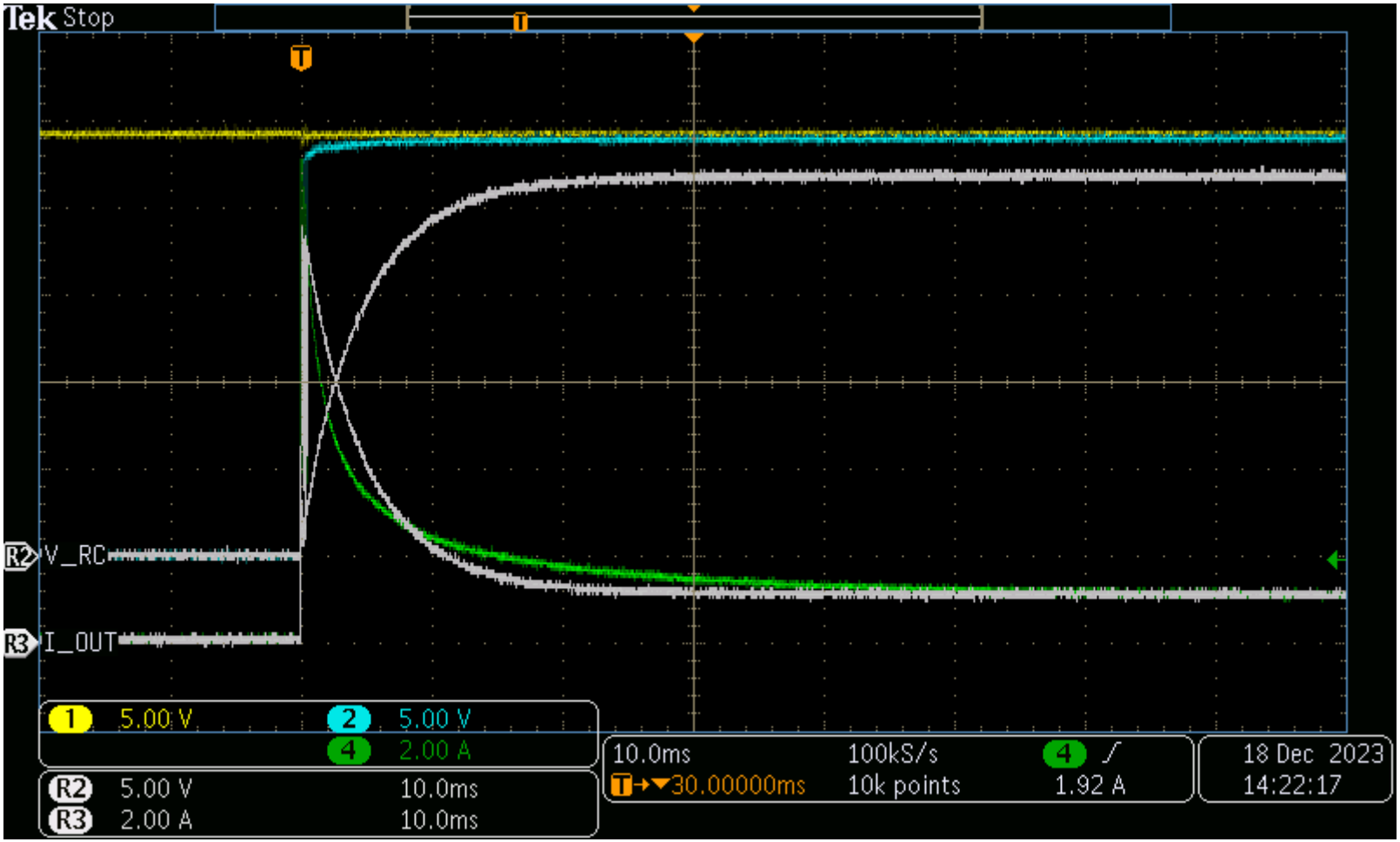

FIGURE C.10: WAVEFORM COMPARISON BETWEEN CAPACITIVE AND INCANDESCENT LOAD WITHOUT CURRENT LIMITATION

Legend: Channel 1→V_{CC}, Channel 2→v_1, Channel 4→i, Channel R1→v_1, Channel R3→i, Channels R1, R3 belong to capacitive load

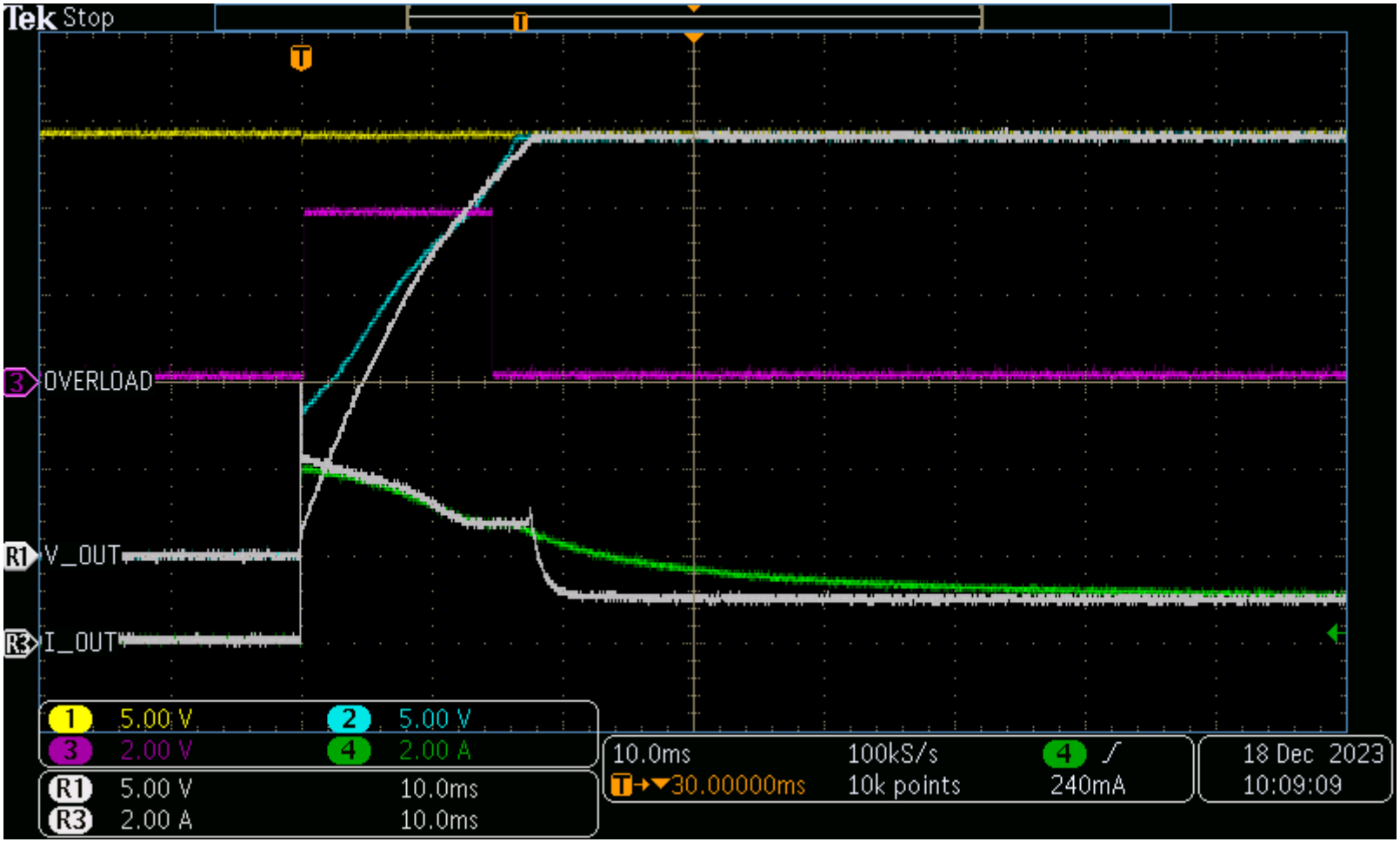

FIGURE C.11: WAVEFORM COMPARISON BETWEEN CAPACITIVE AND INCANDESCENT LOAD WITH CURRENT LIMITATION

Legend: Channel 1→V_{CC}, Channel 2→v_1, Channel 4→i

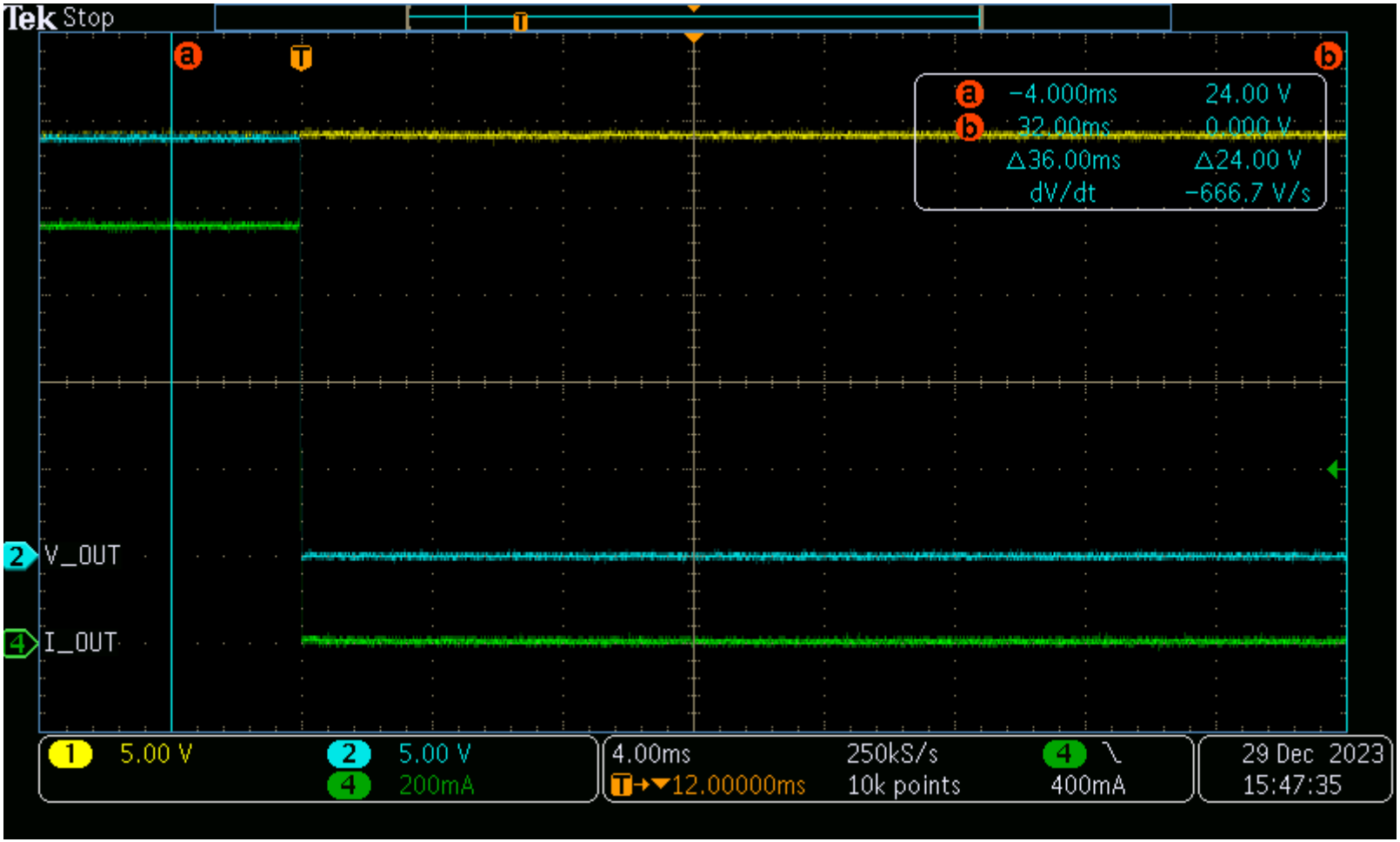

FIGURE C.12: SWITCHING 1A INCANDESCENT LIGHT BULB OFF

List of Figures

List of Tables